
1 Synergistic effects of previous winter NAO and ENSO 2 on the spring dust activities in North China

3 Falei Xu¹, Shuang Wang¹, Yan Li², and Juan Feng¹

4 ¹State Key Laboratory of Remote Sensing Science, Faculty of Geographical Science, Beijing
5 Normal University, Beijing, China

6 ²Key Laboratory for Semi-Arid Climate Change of the Ministry of Education, College of
7 Atmospheric Sciences, Lanzhou University, Lanzhou, China

8 **Correspondence:** Juan Feng (fengjuan@bnu.edu.cn)

9 Abstract

10 ~~Dust plays an important role in influencing~~Dust significantly influences global weather and climate
11 by impacting the Earth's radiative balance. Based on the reanalysis datasets, ~~the impacts of~~
12 ~~preceding winter, this study explores how the~~ North Atlantic Oscillation (NAO) and El Niño-
13 Southern Oscillation (ENSO) ~~enduring the preceding winter impact~~ the following spring dust
14 activities ~~overin~~ North China ~~are explored.~~ It is found that both the NAO and ENSO ~~exert~~
15 ~~significant effects on~~significantly affect dust activities in North China, especially during their
16 negative phases. When both of them are in the negative phases, their combined impact on dust
17 activities exceeding that of either factor individually. The previous winter NAO ~~exhibits significant~~
18 ~~impacts on~~notably affects the sea surface temperatures (SST) in the North Atlantic, associated with
19 an anomalous SST tripole pattern. These SST anomalies ~~can~~ persist ~~to~~into the following spring due
20 to their inherent persistence, ~~when inducing~~ anomalous atmospheric teleconnection wave ~~trains~~
21 ~~would be induced, thereby influencing the~~ train that influence dust activities in North China. ENSO,
22 on the one hand, directly impacts dust activities in North China by modulating the circulation in the
23 Western North Pacific ~~(WNP). Additionally. Moreover,~~ ENSO enhances the NAO's effect on the
24 North Atlantic SST, explaining their synergistic effects on ~~the~~ dust activities ~~overin~~ North China.
25 This study elucidates the combined roles of NAO and ENSO ~~on the~~in influencing dust activities
26 ~~overin~~ North China, providing one season ahead signals for predicting spring dust activities in North
27 China.

1. Introduction

Dust, one of the most significant natural aerosols in the atmosphere, is of great importance to the global radiative balance with its light-absorbing properties, exerting a crucial role in climate change (Lou et al., 2017; Kok et al., 2023). ~~Moreover~~Additionally, dust impacts not only ~~influences~~ its source regions but also extends its ~~impact~~influence across oceans ~~via~~through teleconnections driven by atmospheric circulation. This transboundary transport affects ocean-atmosphere interactions and ~~has a profound impact on~~profoundly impacts the Earth's climate system (Huang et al., 2015). Dust activities, resulting from regional dust surges, ~~poses a~~pose formidable ~~threat~~threats to socio-economic development, natural ~~ecological-environment~~ecosystems, as well as human health and safety (Zhao et al., 2020; Li et al., 2023). The Gobi Desert in East Asia, particularly the Mongolian Plateau and Northern China, is a major source of dust (Chen et al., 2023), contributing approximately 70% of Asia's total dust emissions (Zhang et al., 2003). Given that China is ~~one of the countries~~ profoundly impacted by dust activities (Fan et al., 2018), exploring the variations in dust activities ~~in~~over China is of ~~significant~~great scientific and practical ~~importance~~significance.

Besides the dust source regions over China (mainly Xinjiang and Inner Mongolia), dust content over North China also ~~exhibited~~exhibits high ~~dust content~~values and ~~significant dust~~strong interannual variability (Liu et al., 2004; Ji and Fan, 2019). Additionally, as a crucial center of politics, economy, and population, it is meaningful to investigate the variations of ~~spring~~ dust activities over North China (30-40°N, 105-120°E) and explore the relevant physical mechanisms. Previous studies have ~~revealed~~shown that the frequency of dust events in China exhibits strong variations, with high frequency from the 1950s to 1970s, low frequency from the 1980s to 1990s, and a notable increase after 2000 (Zhu et al., 2008; Ji and Fan, 2019). On interdecadal time scales, climate oscillations such as the Atlantic Multidecadal Oscillation (AMO), Pacific Decadal Oscillation (PDO), and Antarctic Oscillation (AAO) can influence ~~the~~ dust activities by affecting the ~~climate~~climatic background. For instance, the positive phase of PDO ~~is favorable for~~reduced~~reduces~~ dust activities by influencing the mid-latitude westerly ~~belt~~regime, leading to weaker dust activities (uplift and deposition) in the Asian region (Gong et al., 2006). The AMO ~~plays a role in~~affecting the global aridification process by altering the thermal properties between land and sea (Huang et al., 2017). Additionally, the AAO may substantially regulate dust activities in China by ~~affecting the frequency of dust in East Asia through~~influencing the interaction of meridional circulations between the Northern and Southern Hemispheres (Ji and Fan, 2019).

On the interannual scale, a weaker East Asian Winter Monsoon is associated with anomalous

61 circulation over the Gobi and Taklamakan deserts, facilitating the transport of dust, consequently
62 increasing dust content in China (Lou et al., 2016). The variations of the sea ice coverage in the
63 Barents Sea ~~can~~ significantly influence the intensity and frequency of dust activities in China by
64 affecting cyclone generation and thermal instability in North China (Fan et al., 2018). The North
65 Atlantic Oscillation (NAO) ~~exert a substantial influence on the~~ substantially impacts spring dust
66 activities in North China by modulating the zonal wave-train from the Atlantic to the Pacific at
67 mid-latitudes in the Northern Hemisphere, and the sea level pressure (SLP) gradient in the Tarim
68 Basin in China (Zhao et al., 2013). On the synoptic scale, the NAO ~~exerts a vital influence~~
69 ~~on~~ influences the emergence and evolution of dust activities in North China by impacting ~~the~~
70 ~~transport of~~ transient wave flux transport and ~~modifying~~ atmospheric circulation (Li et al., 2023).
71 Beyond extratropical signals, tropical variabilities, such as El Niño–Southern Oscillation (ENSO),
72 also significantly ~~modulated~~ modulate dust activities ~~in China~~ by regulating ~~variations in~~ large-scale
73 circulation, precipitation, and temperature variations over East Asia (Yang et al., 2022), Saudi
74 Arabia (Yu et al., 2015), and North America (Achakulwisut et al., 2017).

75 From the aforementioned studies on ~~the~~ dust activities in China, it is evident that the NAO and
76 ENSO are two important factors, with a focus on their individual effects on the dust activities in
77 China. However, as significant climate variabilities in the extratropical and tropical regions,
78 respectively, the NAO and ENSO often co-occur and have complex interactions (López-Parages et
79 al., 2015). It is found that ENSO can influence the climate near the North Atlantic through
80 atmospheric forcing of the Pacific-North America teleconnection (Wallace and Gutzler, 1981).
81 During the early winter of El Niño events, strong convective anomalies in the tropical Indian Ocean-
82 Western Pacific (Abid et al., 2021) and the Gulf of Mexico-Caribbean Sea (Ayarzagüena et al., 2018)
83 can trigger Rossby wave ~~trains~~ train reaching the North Atlantic, leading to positive NAO signals.
84 Furthermore, the stratosphere, serving as an energy transmission channel, may also be an important
85 pathway for ENSO to influence the NAO (Jiménez-Esteve and Domeisen, 2018). Moreover,
86 observations and numerical simulations have demonstrated that the NAO ~~signal~~ can induce a Gill-
87 Matsuno pattern in the tropical region ~~of southern Eurasia, inducing a decadal enhancement in,~~
88 strengthening the linkage connection between the East Asian Summer Monsoon and ENSO (Wu et
89 al., 2012). When the NAO is in its positive phase, intensified northeasterlies ~~are observed~~ over
90 tropical North Atlantic, ~~resulting in increased~~ are observed, increasing low-level moisture content
91 and precipitation in the tropical North Atlantic, ~~paralleling with stronger convection and enhanced~~
92 ENSO which in turn enhances ENSO's impact (Ding et al., 2023). These studies highlight emphasize
93 the connections and interactions between NAO and ENSO, underscoring the necessity of

94 considering their synergistic effects on the dust activities in North China.

95 The synergistic effect refers to the phenomenon where the combined impacts of two or more
96 factors are significantly greater than their individual roles (Li et al., 2019). It has been found that
97 there are synergistic effects in the impact of NAO and ENSO on the weather and climate in China.
98 The NAO can facilitate the development of the subpolar teleconnection across northern Eurasia
99 downstream, leading to anomalies in the high-pressure systems over the Ural Mountains and the
100 Sea of Okhotsk, which in turn affect the East Asian Summer Monsoon (Wang et al., 2000).
101 Meanwhile, ENSO exerts significant impact on the convective activities in the central Pacific and
102 induces alterations in the equatorial circulation via the Pacific-East Asia teleconnection, further
103 affecting the atmospheric circulation and sea surface temperature (SST) in the Western North Pacific
104 (WNP), ultimately influencing the intensity of the East Asian Summer Monsoon (Wang et al., 2000).
105 Therefore, the synergistic effects of ~~these factors~~ NAO and ENSO can result in pronounced impacts
106 on the East Asian Summer Monsoon. During El Niño events, SST in the central and eastern
107 equatorial Pacific rises, enhancing convective activity near the equator, which brings more moisture
108 to Northern China and increases the likelihood of precipitation. Simultaneously, the positive phase
109 of NAO can alter atmospheric pressure in the North Atlantic, influencing atmospheric circulation
110 over the Eurasian continent. ~~This interaction between~~ The influences of NAO and ENSO
111 synergistically ~~regulates, to some extent, regulate~~ the distribution of precipitation in Northern China
112 (Guo et al., 2012).

113 The synergistic effects of NAO and ENSO significantly influence the climate in China, but
114 their synergistic effects on the spring dust activities over North China and the mechanisms involved
115 remain unclear. This study will investigate these effects on dust activities over North China,
116 providing a scientific foundation for predicting dust activities in China. The structure of this paper
117 is as follows: Section 2 outlines the datasets and methods employed in this study. Section 3 presents
118 the analysis and findings. Section 4 contains the conclusions and discussions.

119 **2. Datasets and methods**

120 **2.1 Datasets**

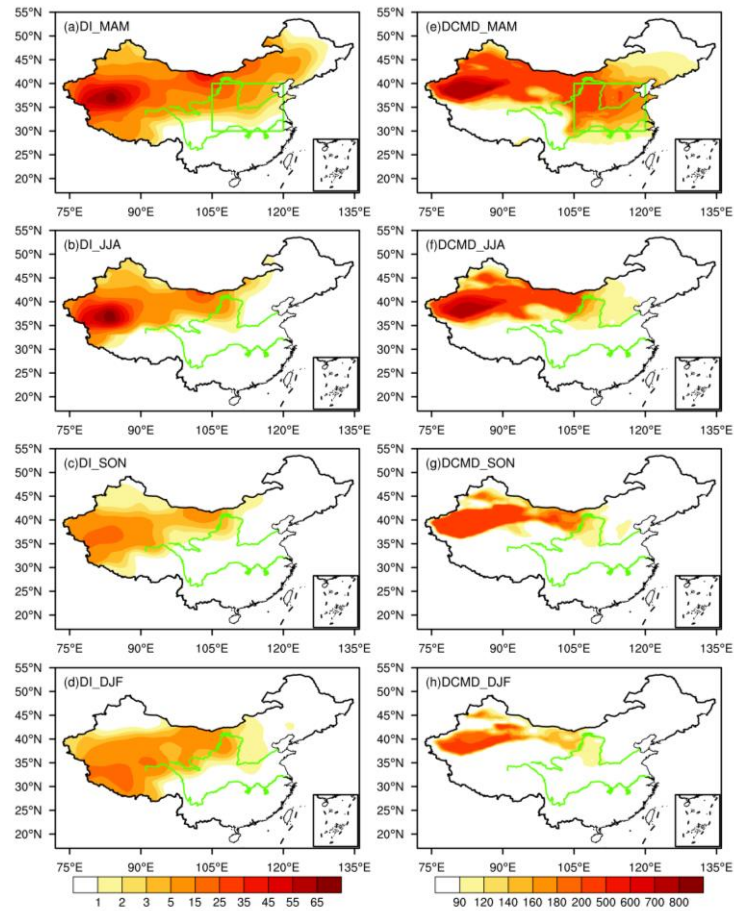
121 The dust dataset for the Modern-Era Retrospective Analysis for Research and Applications
122 Version 2 (MERRA-2) was obtained from NASA's Global Modeling and Assimilation Office
123 (GMAO), incorporating assimilated observations from both satellites and ground stations (Gelaro
124 et al., 2017). In this study, the Dust Column Mass Density of the MERRA-2 `tavg1_2d_aer_Nx`

product was utilized to represent the dust content with a $0.5^\circ \times 0.625^\circ$ resolution from 1980-2022. Previous studies have demonstrated the applicability of MERRA-2 reanalysis data for representing the spatiotemporal distribution characteristics of dust content in China (Kang et al., 2016; Wang et al., 2021). It is reported that the ~~result~~results based on MERRA-2 are similar to those obtained from MODIS, OMPS, CALIPSO, and Himawari-8 ~~data~~datasets (Kang et al., 2016; Wang et al., 2021). Additionally, we further employ the datasets from the China National Meteorological Centre from 1980-2018, which include observations of floating dust, blowing dust, and dust storms, to validate the reliability of MERRA-2 reanalysis ~~data~~dataset. The frequency of dust activities recorded at these stations has been converted into a Dust Index (DI) (Wang et al., 2008; Equations 1), effectively representing the dust content.

$$DI = 9 \times DS + 3 \times BD + 1 \times FD \quad (1)$$

Where DS, BD, and FD represent the frequency of dust storms, blowing dust, and floating dust, respectively. Additionally, DI denotes the dust content ~~of dust aerosols~~ at each station. It is worth noting that the value of 1 represents the normalized mass weight of dust content for each FD, while 3 and 9 represent the relative mass weight of dust content for BD and DS, respectively (Wang et al., 2008). Therefore, DI is an index used to indicate the dust content which does not have unit. In order to better compare the DI with the reanalysis, we first interpolate the site data into grid points by Cressman (1959), and then obtain the gridded DI. We found that the ~~variations~~distribution of ~~the~~ DI and MERRA-2 dust ~~aerosols~~ content during the four seasons all show similar spatial characteristics (Figure 1). The above results indicate that the MERRA-2 reanalysis data can capture the spatiotemporal characteristics of dust content in China, which is applicable to understand the variations in dust content in China.

Additionally, the SST dataset was derived from the Hadley Centre of the UK Met Office on a $1^\circ \times 1^\circ$ grid (Rayner et al., 2003). The atmospheric reanalysis datasets employed herein were provided from the Fifth Generation Reanalysis Version 5 (ERA-5) of the European Centre for Medium-Range Weather Forecasts (ECMWF) with a resolution of $0.25^\circ \times 0.25^\circ$ on 37 vertical levels (Hersbach et al., 2020). The period of SST and atmospheric reanalysis datasets was from 1979-2022. The winter is defined as the average of December-February (December-January-February, DJF), with the winter 1979 (2021) corresponding to the average of December in 1979; (2021), January and February in 1980 (2022). The spring seasonal mean is the average of March, April, and May. Thus, the previous winter is from 1979 to 2021, and the following spring is from 1980 to 2022. To focus the investigation into the interannual variability, the linear trends of all variables were



158

159 **Figure 1.** (a-d) Spatial distribution of seasonal mean DI based on station data, (e-h) as in (a-d), but
 160 for dust column mass density based on MERRA-2 (units: $\text{mg}\cdot\text{m}^{-2}$). The green box in (a) and (e)
 161 represents North China. The green lines represent the Yellow River (northern one) and the Yangtze
 162 River (southern one), respectively.

163 2.2 Methods

164 The NAO index (NAOI) used is following Li and Wang (2003), quantified by the difference in
 165 the normalized monthly SLP regionally zonal averaged over the North Atlantic within 80°W - 30°E
 166 between 35°N and 65°N . This definition effectively captures the large-scale circulation
 167 characteristics associated with NAO, essentially measuring the intensity of zonal winds spanning
 168 the entire North Atlantic. We also employed the NAOI ~~produce by from~~ Hurrell (1995) and Jones
 169 (1997), ~~which have been used in many studies (e.g.,) to validate the NAOI by~~ Li and Wang (2003).
 170 A good agreement with correlation coefficients of 0.96 and 0.94 between these two indices and the
 171 NAOI defined by Li and Wang (2003). Furthermore, ENSO is characterized by Niño3.4 index with
 172 SST anomalies averaged over 5°S - 5°N , 170°W - 120°W (Trenberth, 1997).

173 In this study, ~~we utilized the seasonal standardized indices of seasonal averages during the~~

174 ~~previous winter (the winter from 1979 to 2021), with values exceeding 0.5 standard~~
 175 ~~deviations~~deviation identified as anomalous years, ~~as shown in Table 1. The winter NAO and ENSO~~
 176 ~~indices are during 1979-2021, and the spring dust are during 1980-2022, to highlight the preceding~~
 177 ~~impacts of previous winter on the following spring.~~ The correlation analysis is used to
 178 ~~explore~~examine the relationship between NAO/ENSO and dust content over North China, ~~and~~
 179 ~~the~~while composite analysis ~~is employed to investigate~~investigates the synergistic effects of these
 180 climatic variabilities on ~~the~~ dust activities over North China. The statistical significance of the
 181 correlation, regression, and composite values ~~was evaluated by~~is assessed using a two-sided
 182 Student's *t*-test. Unless otherwise noted, all reported statistically significant levels are at the 0.1
 183 level.

184 The memory effect of SST can be elucidated by the SST persistence component (SST_p), as
 185 delineated in equation (2) (Pan, 2005).

$$186 \quad SST_p = SST(t) * \frac{Cov[SST(t), SST(t + 1)]}{Var[SST(t)]} \quad (2)$$

187 SST_p represents the memory effect of the previous SST (t : ~~previous winter~~) on the following SST
 188 ($t + 1$: ~~spring~~), where $SST(t)$ and $SST(t + 1)$ denote the previous winter SST and spring SST,
 189 respectively. $Cov[SST(t), SST(t + 1)]$ denotes the covariance between the previous winter SST
 190 and spring SST, while $Var[SST(t)]$ signifies the variance of the previous winter SST.
 191 Consequently, the $Cov[SST(t), SST(t + 1)]/Var[SST(t)]$ represents the connection between the
 192 SST variations in previous winter and spring. A greater value of SST_p indicates the variation of
 193 $SST(t + 1)$ is more closely attached with the variation of $SST(t)$.

194 The T-N wave activity flux (WAF), formulated by Takaya and Nakamura (2001), represents a
 195 three-dimensional wave action flux that describes the energy dispersion characteristics of stationary
 196 Rossby waves, thereby reflecting the direction of Rossby wave energy dispersion. The WAF is
 197 suitable for application in mid-high latitude regions where the background circulation deviates from
 198 uniform zonality, as obviates the need for the assumption that the basic flow field must be a zonally
 199 averaged basic flow and can accommodate zonally non-uniform wind fields. The convergence and
 200 divergence characteristics of WAF reveal the source and dissipation areas of wave energy, with the
 201 transmission direction ~~being interpretable as~~indicating the direction of energy transport. The three-
 202 dimensional formulation of WAF is as follows:

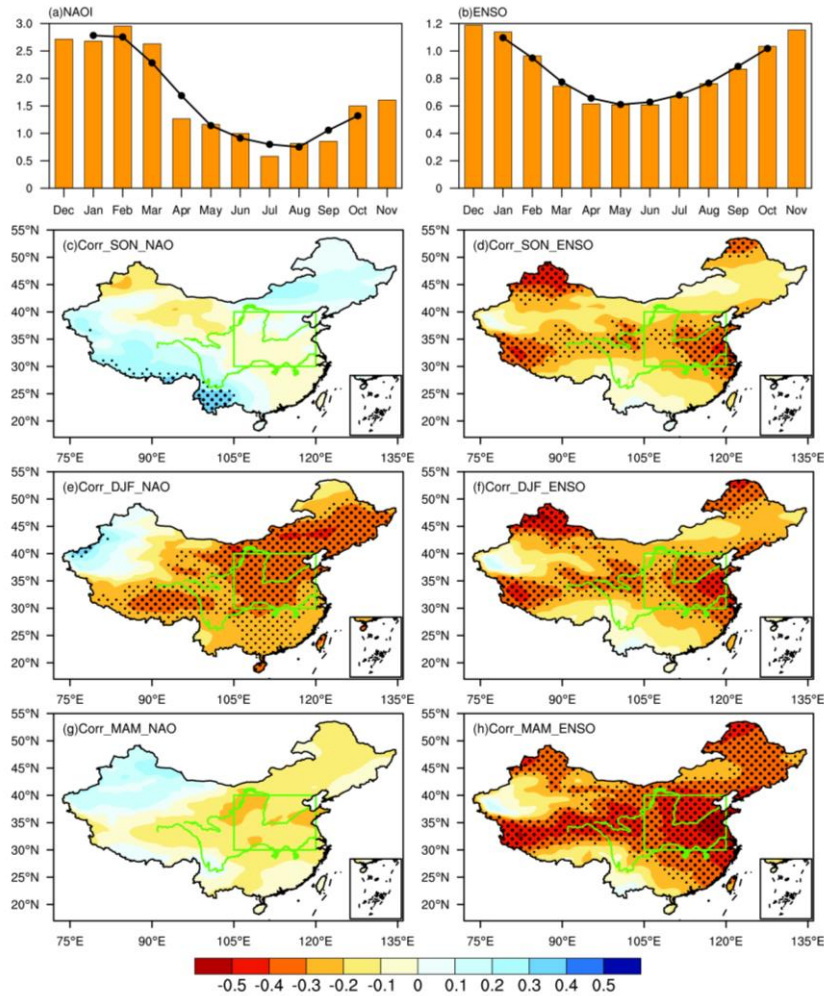
$$W = \frac{p \cos \varphi}{2|U|} \cdot \left(\begin{array}{l} \frac{U}{a^2 \cos^2 \varphi} \left[\left(\frac{\partial \psi}{\partial \lambda} \right)^2 - \psi \cdot \frac{\partial^2 \psi}{\partial \lambda^2} \right] + \frac{V}{a^2 \cos \varphi} \left[\frac{\partial \psi}{\partial \lambda} \frac{\partial \psi}{\partial \varphi} - \psi \cdot \frac{\partial^2 \psi}{\partial \lambda \partial \varphi} \right] \\ \frac{U}{a^2 \cos \varphi} \left[\frac{\partial \psi}{\partial \lambda} \frac{\partial \psi}{\partial \varphi} - \psi \cdot \frac{\partial^2 \psi}{\partial \lambda \partial \varphi} \right] + \frac{V}{a^2} \left[\left(\frac{\partial \psi}{\partial \varphi} \right)^2 - \psi \cdot \frac{\partial^2 \psi}{\partial \varphi^2} \right] \\ \frac{f_0^2}{N^2} \left\{ \frac{U}{a \cos \varphi} \left[\frac{\partial \psi}{\partial \lambda} \frac{\partial \psi}{\partial z} - \psi \cdot \frac{\partial^2 \psi}{\partial \lambda \partial z} \right] + \frac{V}{a} \left[\frac{\partial \psi}{\partial \varphi} \frac{\partial \psi}{\partial z} - \psi \cdot \frac{\partial^2 \psi}{\partial \varphi \partial z} \right] \right\} \end{array} \right) \quad (3)$$

204 In the expression, p , φ , λ , f_0 , and a represent the geopotential height atmospheric pressure,
 205 latitude, longitude, ~~coriolis~~Coriolis parameter, and Earth's radius, respectively. $\psi' = \Phi' / f f_0$
 206 (where Φ represents the geopotential height) denotes the disturbance of the quasi-geostrophic
 207 stream function relative to the climatology. N is buoyancy frequency, $z = -H \ln(p)$ with H
 208 being a constant scale height ($H=8$ km). The basic flow field $\mathbf{U} = (U, V, Z)$ (where Z
 209 represents the selected level) denotes the climatic field, where U and V indicate the zonal and
 210 meridional velocities, respectively.

211 3. Results

212 3.1 Impacts of NAO and ENSO on the spring dust in North China

213 The NAO shows the strongest variability during the winter months, with the maximum
 214 standard deviation of the NAO peaks during December, January, and in February. By analyzing the
 215 three-month running average standard deviation, it is seen the maximum occurs during winter. This
 216 indicates that winter NAO exhibits stronger variability compared to other seasons (Figure 2a).
 217 Similarly, ENSO shows larger variation during winter (Figure 2b). Previous studies have found that
 218 preceding NAO and ENSO play important roles in impacting significantly impact the
 219 following subsequent climate over North China, particularly the cross-seasonal impacts (Zheng et
 220 al., 2016a; Feng et al., 2019). We have examined the roles of the previous autumn, winter and
 221 simultaneous spring NAO and ENSO on the spring dust aerosols-over North China. It is found that
 222 the most significant influences of NAO and ENSO on the on spring dust aerosols occurs occur when
 223 the-NAO and ENSO leading lead by one season (Figures 2c-h). Therefore, the roles impacts of the
 224 previous winter NAO and ENSO on the-spring dust aerosols-over North China are discussed in the
 225 study.

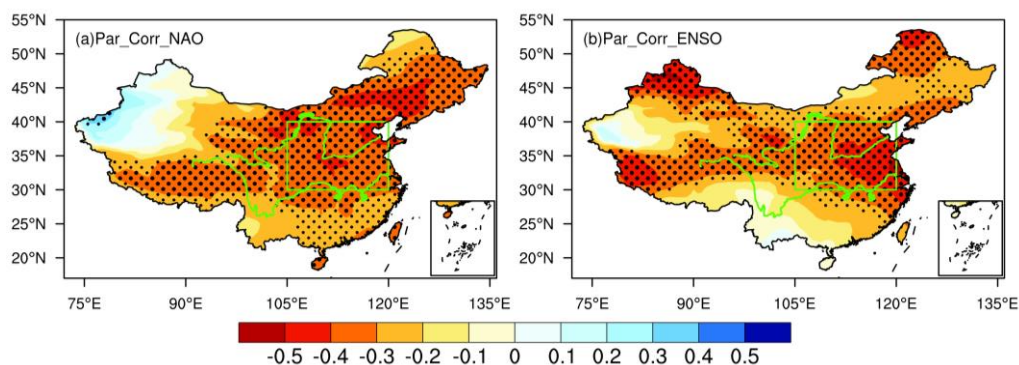


226

227 **Figure 2.** The monthly standard deviation of (a) NAOI and (b) Niño3.4 index, respectively. Black
 228 line represents three-month running average of standard deviation. (c) Spatial distribution of
 229 correlation coefficients between the previous autumn NAOI and spring dust content . (d) As in (c),
 230 but with Niño3.4 index. (e-f) and (g-h), as in (c-d), but for the correlations with previous winter and
 231 simultaneous spring NAOI and Niño3.4 index, respectively. The green box represents North China.
 232 Thick and fine stippled areas are statistically significant at the 0.05 and 0.1 level, respectively. The
 233 green lines in (c-h) represent the Yellow River (northern one) and the Yangtze River (southern one),
 234 respectively.

235 The results indicate that lower (higher) dust content is expected when the NAO and ENSO are
 236 in the positive (negative) phases (Figures 2e-f). Meanwhile, the NAOI/Niño3.4 index is significantly
 237 correlated with the areal-area-averaged spring dust content over North China (SDI), with correlation
 238 coefficient coefficients of -0.36/-0.35, statistically significant at the 0.1 level. Considering the
 239 significant interaction relationship between the NAO and ENSO (López-Parages et al., 2015; Zhang
 240 et al., 2015), to detect their independent effects on the dust content, the partial correlation between
 241 NAO (ENSO) and dust content after removing the influence of the ENSO (NAO) are is provided:
 242 (Figures 3a-b). The results indicate that the significant correlation regions between dust content and

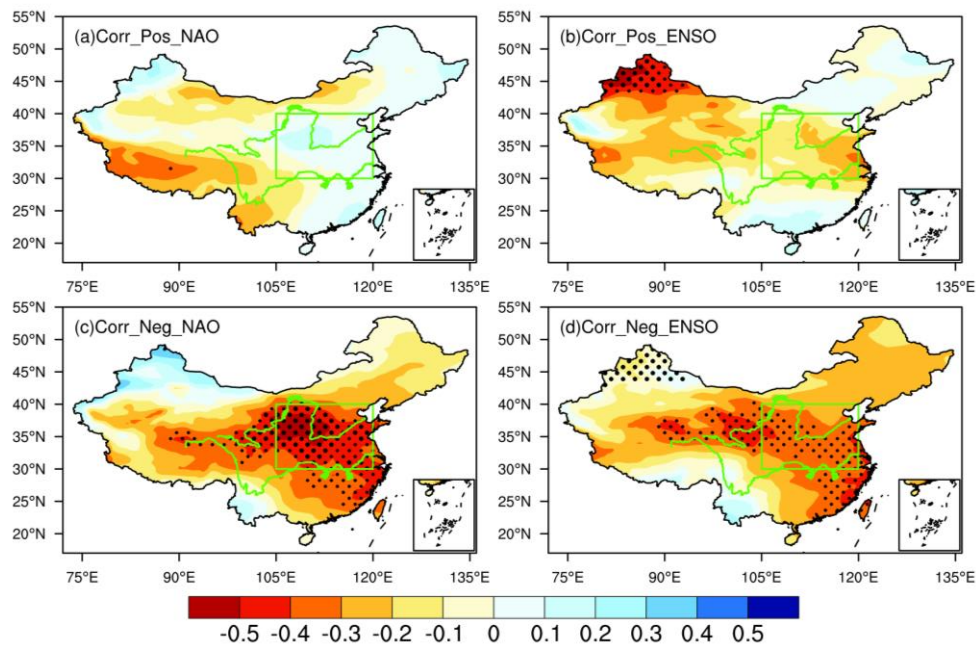
243 either ~~the~~ NAO or ENSO show little change after removing the influence of the other. These findings
 244 suggest a stable and significant connection between the previous winter NAO ~~and~~ / ENSO and ~~the~~
 245 ~~dust content in North China (Figures 3e-d)~~. SDI.



246
 247 **Figure 3.** (a) Spatial distribution of partial correlation coefficients between the previous winter
 248 NAOI and spring dust content. (b) ~~As in (a), but with Niño3.4 index.~~ (c) ~~As in (a), but for the partial~~
 249 ~~correlation~~ after removing the effect of ENSO. (d) ~~As in (ea), but for correlation between Niño3.4~~
 250 ~~index and dust content~~ after removing the effect of NAO. The green box represents North China.
 251 Thick and fine stippled areas are statistically significant at the 0.05 and 0.1 level, respectively. The
 252 green lines represent the Yellow River (northern one) and the Yangtze River (southern one),
 253 respectively.

254 Previous studies have indicated that the development rate, intensity variations, and ~~the~~ spatial
 255 structure of ~~the~~ NAO exhibit distinct ~~asymmetric characteristics~~ asymmetries between different
 256 phases (Feldstein, 2003; Jia et al., 2007). ~~Furthermore, And~~ the influence of NAO on the East Asian
 257 Winter Monsoon is more pronounced during its negative phase (Sung et al., 2010). ~~Similarly, both~~
 258 ~~observational facts and model experiments suggest~~ In addition, it is shown that El Niño and La Niña,
 259 as the positive and negative phases of ENSO, are not simply mirror images of each other. The SST
 260 anomalies in the tropical Pacific associated with ENSO exhibit significant ~~asymmetry~~ asymmetries
 261 ~~in terms of~~ meridional range (Zhang et al., 2009), amplitude (Su et al., 2010), zonal propagation
 262 (McPhaden and Zhang, 2009), ~~as well as climate impact and impacts~~ (Feng and Li, 2011; Feng et
 263 al., 2020) under El Niño and La Niña conditions. ~~Consequently, we To~~ further explore these
 264 asymmetries, we analyzed the connection between NAO/ENSO and ~~spring dust but in~~ SDI during
 265 different phases. The results indicate that the relationship between NAO/ENSO and ~~dust in North~~
 266 ~~China~~ SDI also exhibits significant asymmetry, i.e., with weaker (stronger) correlations during their
 267 positive (negative) phases ~~of NAO and ENSO~~ (Figure 4), ~~where significant correlations only appear~~
 268 ~~in the negative phases of NAO and ENSO~~. Based on the scatter distribution of SDI under different
 269 phases of NAO and ENSO, it is noted that the correlation coefficients between NAOI and SDI
 270 during the positive and negative phases of NAO are ~~-0.46~~ 05 (statistically insignificant) and ~~-0.05~~,

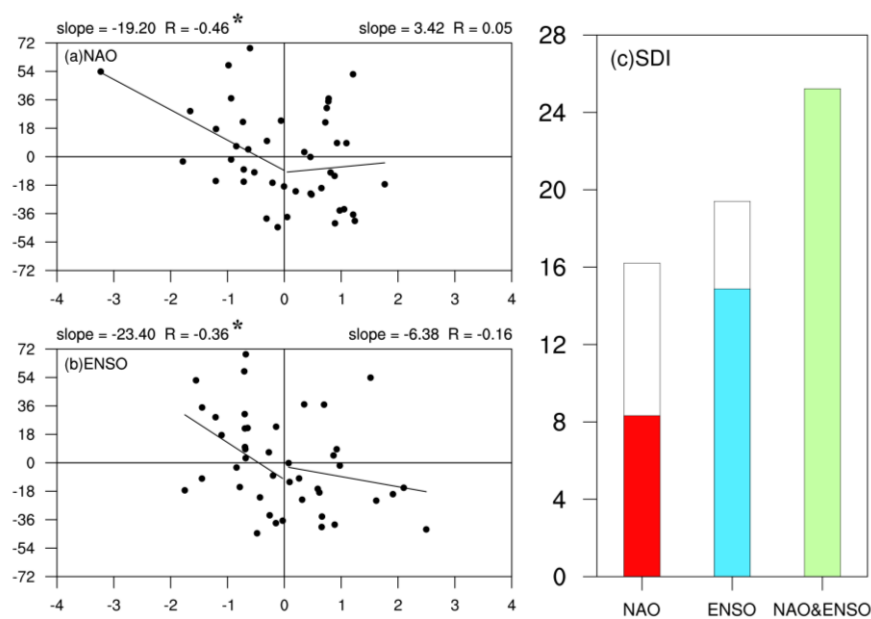
271 respectively, 46 (statistically significant), indicating that the significant influence of NAO on the
 272 dust in North China SDI mainly occurs during its negative phase (Figure 5a). Similarly, the
 273 correlation distribution coefficients between ~~the~~ ENSO and SDI also shows that the influence of
 274 ENSO is more pronounced during its negative phase, with the correlation coefficients for the
 275 positive and negative phases being -0.16 (statistically insignificant) and -0.36 (statistically
 276 significant), respectively (Figure 5b). These results indicatedemonstrate that the impacts of the
 277 previous winter NAO and ENSO on the spring dust content in North China SDI exhibit asymmetrical
 278 characteristics, with significant effects mainly primarily manifested during their negative phases. —



279
 280 **Figure 4.** Spatial distribution of correlation coefficients between (a) positive and (c) negative NAO
 281 phases and dust content. (b) and (d) as in (a) and (b), respectively, but for the Niño3.4 index. The
 282 green box represents North China. Thick and fine stippled areas are statistically significant at the
 283 0.05 and 0.1 level, respectively. The green lines represent the Yellow River (northern one) and the
 284 Yangtze River (southern one), respectively. —

285 The synergistic effects of climate variabilities from mid-high latitudes and the tropics are
 286 pivotal mechanisms affecting the weather and climate in East Asia (Feng et al., 2019; Li et al., 2019).
 287 Correspondingly, we will examine whether the negative phases of the previous winter NAO and
 288 ENSO exert synergistic effects on the following spring dust content inover North China. As shown
 289 in Figure 5c, when the NAO is in its negative phase (Table 1; white bar in Figure 5c labeled NAO),
 290 the value of anomalous dust content over North China SDI is $+16.21 \text{ mg} \cdot \text{m}^{-2}$, (statistically
 291 significant), whereas it is $+8.32 \text{ mg} \cdot \text{m}^{-2}$ (statistically insignificant) for the case that negative NAO
 292 occurred alone (red bar in Figure 5c). Similarly, the value of dust content anomalies over North
 293 Chinaanomalous SDI in the negative ENSO phase is greater than that when negative ENSO

294 occurred alone ($+19.40 \text{ mg}\cdot\text{m}^{-2}$ (statistically significant) vs. $+14.88 \text{ mg}\cdot\text{m}^{-2}$ (statistically
 295 insignificant)). When both the NAO and ENSO both are in their negative phases (Table 1), the value
 296 of ~~dust content anomalies~~ anomalous SDI ($+25.23 \text{ mg}\cdot\text{m}^{-2}$; statistically significant) is much greater
 297 than the situation when one of them is in the negative phase (green bar in Figure 5c). That is This
 298 indicates that the negative phases of the previous winter NAO and ENSO demonstrate synergistic
 299 effects on the ~~spring dust activities in content over~~ North China. Therefore, three categories, i.e., the
 300 NAO ~~(/ ENSO)~~ is in its negative phase, and both the NAO and ENSO are in the negative phases
 301 ~~simultaneously~~ (Table 1) are discussed in the context, to elucidate the relevant processes of the
 302 synergistic effects of NAO and ENSO on the dust content over North China. –



303
 304 **Figure 5.** Scatterplots of the spring dust content in North China against previous winter (a) NAOI
 305 and (b) Niño3.4 index. Also shown are lines of best fit for positive and negative NAOI/Niño3.4
 306 index values and correlation coefficients (R), slope (slope), * indicates statistically significant at the
 307 0.1 level. (c) Spring dust content over North China during the negative NAO, negative ENSO phases,
 308 and concurrent negative phases of NAO and ENSO (unit: $\text{mg}\cdot\text{m}^{-2}$). White bars represent negative
 309 phases of the NAO and ENSO, red and blue bars indicate solo negative NAO and ENSO years, and
 310 green bar is the negative NAO and ENSO co-occurring years. –

311 **Table 1.** The events of NAO and ENSO classified by three categories

| Scenarios | Years | Numbers |
|--------------------------------------|---|---------|
| NAO ⁻ | 1980,1982,1985,1986,1987,1996,1998,2001, 2003,2004,2006,2010,2011,2013,2021 | 15 |
| ENSO ⁻ | 1984,1985,1986,1989,1996,1999,2000,2001, 2006,2008,2009,2011,2012,2018,2021,2022 | 16 |
| NAO ⁻ & ENSO ⁻ | 1985,1986,1996,2001,2006,2011,2021 | 7 |

3.2 Impacts of NAO and ENSO on the environmental variables

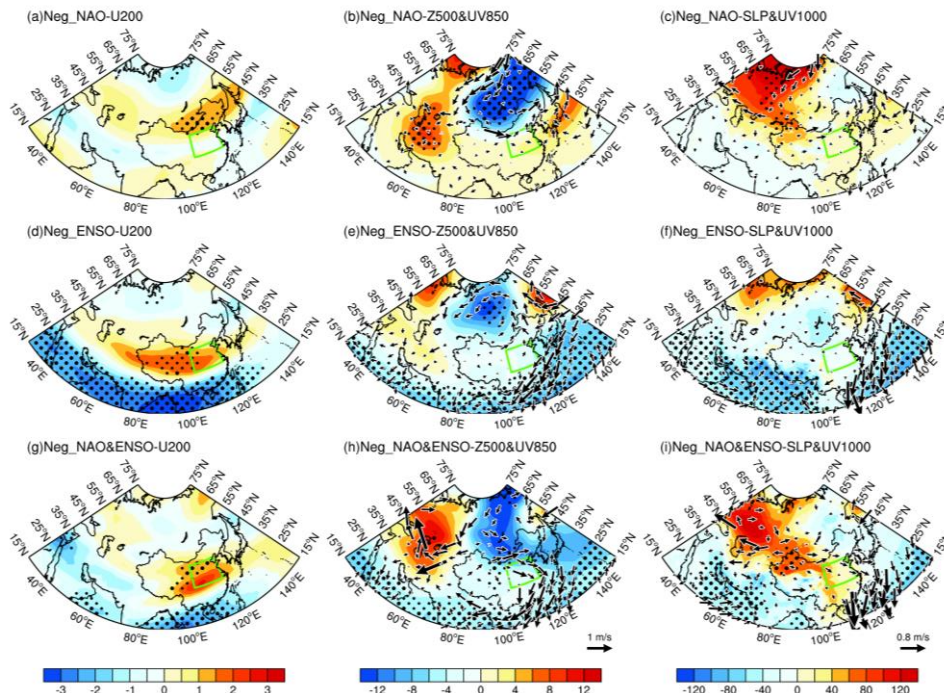
To examine the anomalous characteristics associated with NAO and ENSO, the circulation anomalies in their negative phases, as well as in their co-occurring negative phases (Table 1) are analyzed. In the upper troposphere (200 hPa), ~~the zonal wind is strengthened~~ intensifies over ~~the northwest of~~ China and Mongolia during the negative NAO phase (Figure 6a), with ~~evident~~ significant positive anomalies centered ~~on~~ over Mongolia. In the ~~case of~~ negative ENSO phase, ~~the upper-level~~ intensified zonal ~~wind also shows an intensification over the~~ winds over northwest ~~region of~~ China and Mongolia are observed in the upper level (Figure 6d). The intensification of upper-level zonal wind boosts the upper-level momentum, which is subsequently transferred downward to the mid-lower troposphere through vertical circulation (Wu et al., 2016; Li et al., 2023), causing windy weather in the ~~surface~~ dust source regions, facilitating dust lifting and transport activities, thereby promoting the occurrence of dust activities in the downstream North China. When both the NAO and ENSO are in their negative phases, the ~~main~~ primary positive anomaly center appears over the northern part of North China, ~~which is stronger than the situation in either the NAO or ENSO. This~~ facilitating dust transport to North China. The result implies the synergistic effects of NAO and ENSO on the upper-level zonal wind, ~~facilitating an enhanced~~ enhancing dust transport ~~of dust from its~~ source regions to North China, ~~consequently triggering the onset of~~ favoring for dust activities ~~conditions~~ in North China (Figure 6g).

Subsequent analysis delved into the anomalous distribution of the circulation field in the mid and lower troposphere. In the negative NAO situation, a pronounced “trough-ridge” anomaly pattern emerges in the mid-latitude region, characterized by a trough in Siberia and a ridge in the Middle East (Figure 6b). This atmospheric configuration fosters a dominant meridional circulation in the mid-high latitude region, ~~thereby facilitating~~ enhancing the ~~enhanced~~ southward transport of cold air from the north. ~~Such a southward~~ This incursion of cold air ~~serves to strengthen the~~ strengthens surface wind speeds, ~~and to promote~~ promoting the uplift and transport of dust from ~~the~~ source regions. In the negative ENSO situation, ~~although the mid-latitude region exhibits~~ a similar trough-ridge pattern; is observed in the mid-latitude, but with more pronounced circulation anomalies ~~are observed~~ over the WNP. ~~At this time, the~~ The region is predominantly under the influence of northeasterly winds on its western flank, manifesting cyclonic circulation anomalies (Figure 6e). This abnormal circulation ~~will hinder~~ hinders the northward transport of warm and moist air from the South China Sea and the Bay of Bengal, diminishing the likelihood of interactions with cold air from the north, thus reducing the ~~possibility~~ likelihood of ~~forming~~ formation of stationary fronts and

344 precipitation. The decrease in precipitation weakens the wet deposition ~~effect~~ (Zheng et al., 2016b;
345 Huang et al., 2021), favoring the occurrence of dust activities in ~~the region~~ North China. When both
346 the NAO and ENSO are ~~simultaneously occurred in their negative phases~~, the meridional circulation
347 in the mid-latitude region is enhanced (Figure 6h). ~~Furthermore, the~~ The southward shift of the
348 trough-ridge pattern ~~leads to a more significant increase in~~ ~~insignificantly increases~~ wind ~~speeds~~ ~~speeds~~
349 in the upstream dust source regions of North China, providing a ~~more~~-substantial source of dust for
350 North China. ~~Meanwhile~~ ~~Additionally~~, the presence of ~~a~~ cyclonic circulation anomalies over the
351 WNP reduces the transport of warm and moist air from the south, which is unfavorable for
352 precipitation, ~~thereby lowering~~. ~~This reduction in precipitation suppresses~~ the wet deposition ~~effect~~
353 ~~on dust and further~~, favoring the ~~onset~~ ~~occurrence~~ and intensification of dust activities in North China.

354 As for the SLP, significant positive ~~SLP~~ anomalies appear in Eastern Europe and Russia during
355 ~~the~~ negative NAO situation, ~~indicative of an intensified~~ ~~indicating the~~ Siberian High (SH), ~~which~~
356 ~~extends~~ ~~is intensified and extended~~ southward to the dust source regions upstream of North China
357 (Figure 6c). The intensification of the SH is typically accompanied ~~by~~ ~~with~~ strong northerlies and
358 dry conditions, ~~favoring~~ ~~which favor~~ the transport of dust, thereby supplying abundant material
359 sources for dust activities in North China. In the negative ENSO case, although the high-latitude
360 region exhibits a weaker SH signal, ~~similar to the ENSO influence on the circulation pattern in the~~
361 ~~middle and lower troposphere~~, ~~more~~-significant circulation anomalies occur over the WNP. This
362 cyclonic circulation anomalies inhibit the northward transport of warm and moist air from the south,
363 leading to unfavorable precipitation conditions in North China (Figure 6f). When both the NAO and
364 ENSO are in their negative phases, the intensify and extent of the SH are more pronounced
365 compared to that when the NAO sole is in negative phase. Additionally, cyclonic circulation
366 anomalies persist over the WNP, which are conducive to the occurrence of dust ~~events~~ ~~activities~~ in
367 North China (Figure 6i).

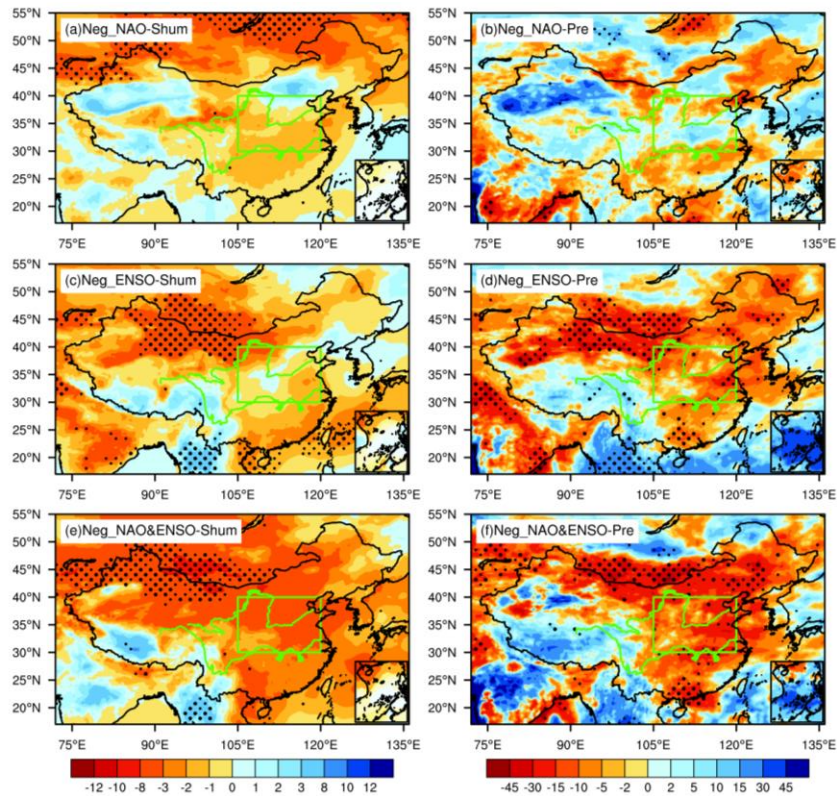
368 The results suggest that when both the NAO and ENSO are in their negative phases, synergistic
369 effects emerge, rendering the atmospheric circulation ~~anomalies~~ in the troposphere more conducive
370 to ~~the occurrence of~~ dust ~~events~~ ~~activities~~ in North China. The synergistic effects ~~may be due to~~ ~~likely~~
371 ~~result from~~ the superposition and interaction of various atmospheric levels ~~and regional~~
372 ~~characteristics~~-modulated by the NAO and ENSO, ~~thereby~~-forming ~~more~~-favorable circulation
373 conditions for dust activities in North China.



374
 375 **Figure 6.** Upper, the composite anomalies of (a) 200 hPa zonal wind (shading, unit: $\text{m}\cdot\text{s}^{-1}$), (b) 500
 376 hPa geopotential height (shading, unit: gpm) and 850 hPa wind field (arrows, unit: $\text{m}\cdot\text{s}^{-1}$), (c) sea-
 377 level pressure (shading, unit: Pa) and 1000 hPa wind field (arrows, unit: $\text{m}\cdot\text{s}^{-1}$) during the negative
 378 NAO phases. Middle-Lower, as in the upper, but during the negative ENSO phases and co-occurred
 379 negative phases of NAO and ENSO, respectively. The green box represents North China. Only wind
 380 anomalies statistically significant at the 0.1 level are shown. Thick and fine stippled areas are
 381 statistically significant at the 0.05 and 0.1 level, respectively.

382 Dust activities are ~~multifaceted phenomena related to~~ not only impacted by large-scale
 383 circulation patterns, and ~~significantly also~~ influenced by local surface conditions and meteorological
 384 processes. Surface properties and local meteorological factors play ~~a role~~ important roles in the initiation,
 385 development, and dissipation of dust activities (Liu et al., 2004; Huang et al., 2021). In particular,
 386 humidity and precipitation ~~play~~ are decisive ~~roles~~ factors in determining the frequency and intensity
 387 of dust activities (Prospero et al., 1987; Kim and Choi, 2015). Low humidity leads to drier soil
 388 conditions in ~~the~~ dust source regions, reducing ~~the~~ soil particle cohesion ~~between soil particles~~ and
 389 facilitating dust lifting and transport ~~activities~~ (Csavina et al., 2014), ~~and vice versa~~. Similarly, ~~the~~
 390 ~~amount of precipitation directly affects the wet deposition process of dust. Less~~ less precipitation
 391 weakens ~~the~~ wet deposition, ~~associated with relatively~~ resulting in higher dust content (Zheng et al.,
 392 2016b). Therefore, we further analyzed ~~the~~ the potential impacts of the NAO and ENSO on ~~the~~
 393 humidity and precipitation. ~~When~~ During the ~~NAO is in its~~ negative NAO phase, humidity and
 394 precipitation slightly decrease in northern northwest China, impacting dust lifting and transport in
 395 the spring dust source regions ~~and North China is generally reduced, particularly in areas near the~~
 396 ~~dust source regions, indicating that these areas are conducive to dust transport and prone to causing~~

397 ~~dust activities in North China (Figure(Figures 7a). As for the precipitation, there is more spring~~
398 ~~precipitation in the northwest region of China, while precipitation in the Mongolia and the North~~
399 ~~China is relatively less (Figure 7b)-.b). In the negative ENSO phase, the ~~variation~~variations in~~
400 ~~humidity ~~is and precipitation are~~ similar to that ~~duringas in~~ the negative NAO-phase, but with a~~
401 ~~greater amplitude (FigureFigures 7c), indicating that ENSO has a stronger impact on the humidity~~
402 ~~conditions in North China. Moreover, the precipitation shows a significant decrease over Mongolia~~
403 ~~and North China, which is highly conducive to dust activities (Figure 7d)-.d). When both the NAO~~
404 ~~and ENSO are in ~~the~~their negative phases, the humidity ~~and precipitation~~ anomalies in the dust~~
405 ~~source regions ~~and North China~~ are more intense than ~~those caused by~~ the individual ~~factor~~factors~~
406 ~~(Figure 7e-h). The ~~variation in precipitation is similar to those in humidity, the reduction in~~~~
407 ~~precipitation in the dust source regions and North China exceeds the sole role (Figure 7f). The~~
408 ~~aforementioned analysis indicates that the~~NAO and ENSO ~~can~~modulate humidity and precipitation
409 ~~by affecting atmospheric circulation anomalies, ultimately affecting dust activities- in North China.~~
410 During the negative NAO case, the diminished atmospheric pressure gradient in the mid-high
411 latitude regions of ~~the~~ North Atlantic leads to the intensification and southward shift of the SH (Zhou
412 et al., 2023), accompanied ~~with~~by strong wind, making the environment drier and conducive to dust
413 lifting and transport in ~~the~~ dust source regions. In the negative ENSO case, the upper atmosphere
414 over the WNP is dominated by significant negative anomalies in geopotential height and
415 northeasterly winds (Zhang et al., 2015), reducing moist ~~air~~ transport. When ~~both~~ the NAO and
416 ENSO ~~both~~ are in ~~their~~ negative phases, their regulation ~~ofon the~~ atmospheric circulation produces
417 synergistic effects, further ~~influencing the variations of humidity and precipitation, thereby~~
418 promoting the occurrence~~and development~~ of dust activities in North China.



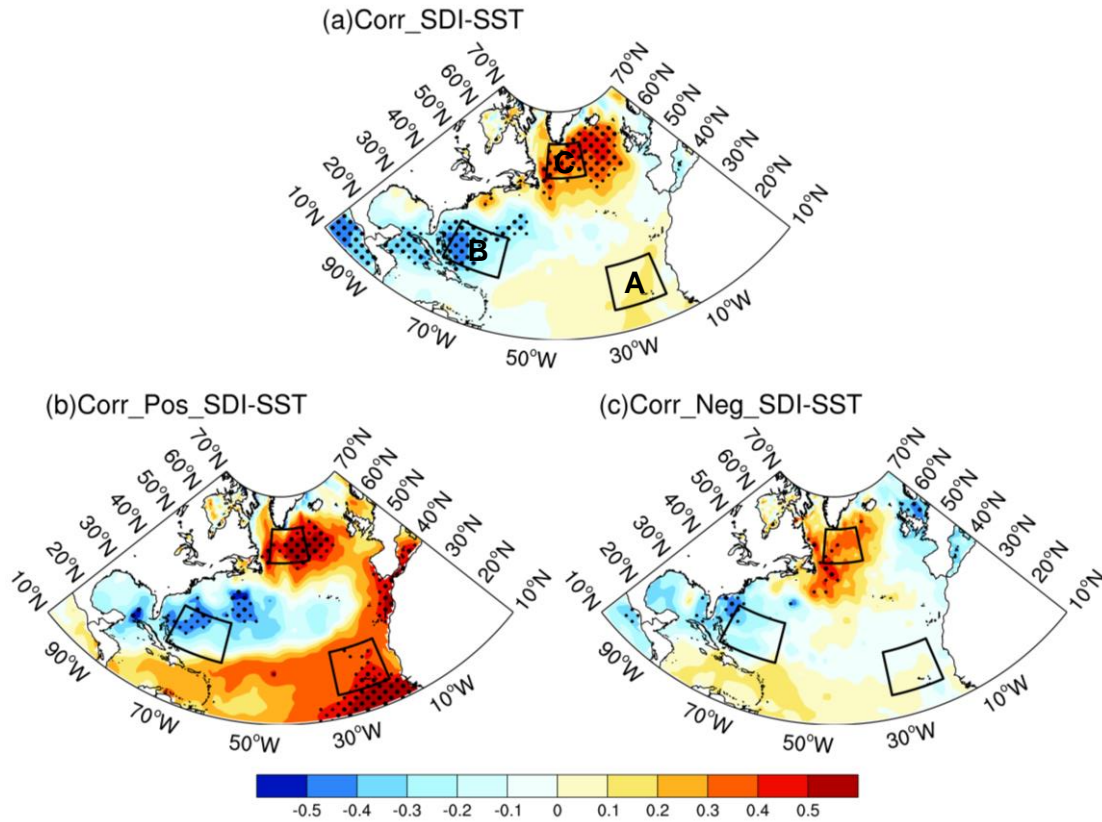
419

420 **Figure 7.** As in Figure 6, but for the composite percentage anomalies of (Left) special humidity and
 421 (Right) precipitation.

422 3.3 Physical Mechanisms of the NAO and ENSO on the dust activities

423 The above results demonstrate that the previous winter NAO and ENSO ~~exert significant~~
 424 ~~impacts on the~~ significantly impact spring dust activities in North China. Consequently, an
 425 examination of the underlying physical mechanisms is warranted. ~~Given the relatively short memory~~
 426 ~~of NAO as an atmospheric phenomenon, we will employ the concept of ocean-atmosphere coupling~~
 427 ~~bridge to elucidate the involved processes.~~ The previous ENSO signal can alter the atmospheric
 428 circulation over the WNP through the persistent impact of SST, ~~thereby significantly~~ affecting
 429 subsequent weather and climate in China (Kim and Kug, 2018; Jiang et al., 2019). ~~Given the~~
 430 ~~relatively short memory of NAO as an atmospheric phenomenon, we will employ the theory of~~
 431 ~~ocean-atmosphere coupling bridge to elucidate the involved processes.~~ The tripole configuration of
 432 SST is the leading mode of SST variation in the North Atlantic, and its variabilities are closely
 433 associated with the NAO (Wu et al., 2009), ~~allowing~~. ~~This association allows~~ the previous NAO
 434 signal to exert a long-term influence on ~~the~~ subsequent weather and climate in China (e.g., Chen et
 435 al., 2020; Wu and Chen, 2020; Song et al., 2022). The variation of ~~the~~ SDI is linked with an
 436 anomalous tripole SST in the North Atlantic (Figure 8a), paralleling ~~with~~ the SST anomalies

437 ~~accompanied~~ associated with the negative phase of ~~the~~ NAO. Therefore, the North Atlantic tripole
 438 index (NATI) is defined to depict the characteristics of SST anomalies (Equations 4-7), ~~as well as~~
 439 ~~the relationships among the NAOI, NATI, and SDI are explored.~~ The correlation analysis between
 440 the high and low years of SDI and ~~NATISST~~ reveals a pronounced difference, indicating an
 441 asymmetric correlation (Figures 8b-c). Specifically, the significant relationship between SDI and
 442 NATI only ~~existed~~ exists in the positive SDI years, ~~with a significant correlation coefficient of -0.47,~~
 443 implying that the occurrence of NATI would ~~connect~~ associate with more dust activities over North
 444 China.



445
 446 **Figure 8.** (a) Spatial distribution of the correlation coefficients between the SDI and simultaneous
 447 SST. (b)-(c) As in (a), but for the positive and negative phases of SDI. Thick and fine stippled areas
 448 are statistically significant at the 0.05 and 0.1 level, respectively. The black box represents NATI.

449
$$\text{SST}_A = [15-25^\circ\text{N}, 32-20^\circ\text{W}] \quad (4)$$

450
$$\text{SST}_B = [22-32^\circ\text{N}, 75-60^\circ\text{W}] \quad (5)$$

451
$$\text{SST}_C = [50-60^\circ\text{N}, 50-32^\circ\text{W}] \quad (6)$$

452
$$\text{NATI} = \text{SST}_B - \frac{1}{2}(\text{SST}_A + \text{SST}_C) \quad (7)$$

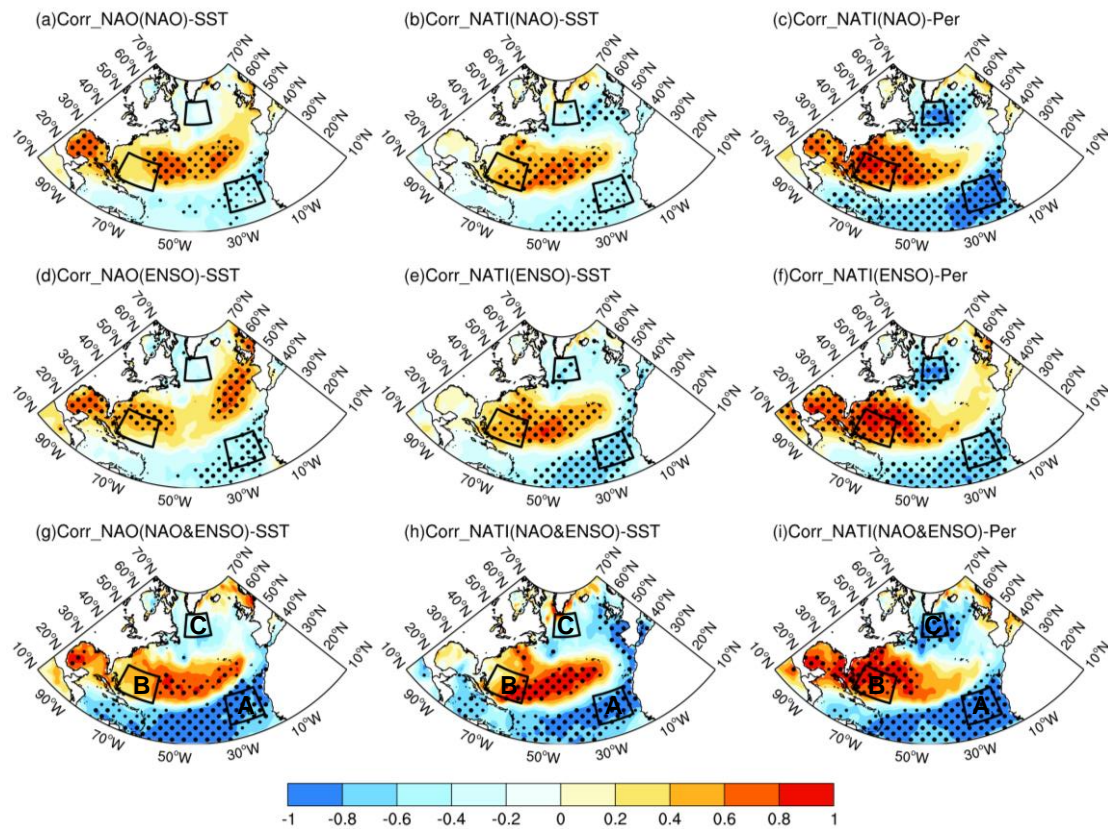
453 ~~Subsequent analyses delved into~~ Moreover, the ~~association~~ relationship between the previous
 454 winter ~~NAO and the North Atlantic SST. It is seen that the correlation coefficients between the~~
 455 ~~negative (positive) NAOI and NATI are -0.41 (-0.09) (figures not shown), indicating that the~~

456 ~~influence of previous winter NAO on the following~~ spring NATI ~~is only manifest~~manifested during
457 ~~the~~ negative phase ~~of NAO, with a statistical significant correlation coefficient of 0.41 (figures~~
458 ~~not shown)~~. This elucidates the reason why the significant impact of NAO on ~~the~~ dust activities in
459 North China only existed during its negative phase. The correlations between the previous winter
460 NAO and North Atlantic SST reveal that NAO is linked with an anomalous tripole SST pattern
461 during the NAO negative situation (Figure 9a). Similar findings are observed during negative ENSO
462 situation (Figure 9d). When both the NAO and ENSO are in their negative phases, the anomalous
463 tripole SST pattern is more pronounced (Figure 9g). This suggests that ENSO enhances the
464 connection between the negative NAO and NATI, providing an explanation for the synergistic
465 effects of the NAO and ENSO on dust activities in North China.

466 In the negative NAO phase, there is a notable correlation between the previous winter NATI
467 and the spring SST and SST_p (Figures 9b-c), indicating that the previous winter NATI can persist
468 into spring, ~~in which~~with the self-persistence of SST playing ~~a crucial~~an important role. Similar
469 findings are observed during the negative ENSO phase ~~of ENSO~~ (Figures 9e-f) and when both the
470 NAO and ENSO ~~occur simultaneously~~ (Figures 9h-i).

471 ~~The correlation between the previous winter NAO and North Atlantic SST reveals that in the~~
472 ~~NAO negative situation (Figure 9a), the variation of NAO is linked with an anomalous tripole SST~~
473 ~~pattern in the North Atlantic. Meanwhile, similar findings are observed during negative ENSO~~
474 ~~situation (Figure 9d). This suggests that there may be positive feedback occurred between NAO and~~
475 ~~North Atlantic SST during negative ENSO phase. When both the NAO and ENSO are in their~~
476 ~~negative phases, the anomalous tripole SST pattern is more pronounced (Figure 9g). This further~~
477 ~~elucidates that ENSO exerts a promoting effect on strengthening the connection between the~~
478 ~~negative NAO and NATI, providing an explanation for the synergistic effects of the NAO and ENSO~~
479 ~~on the dust activities in North China. (Figures 9h-i).~~ Additionally, the correlation coefficients
480 between the NAOI and NATI under different scenarios can illustrate the synergistic influence of the
481 NAO and ENSO on the persistence of SST anomalies (Table 2). Specifically, when the negative
482 ~~phase~~phases of NAO and ENSO ~~co-occur together~~, the correlation coefficients between the NAOI
483 and NATI are greater than those influenced by a single factor alone ~~(Table 2)~~. The impacts of
484 previous winter NAO on the spring dust activities over North China are mainly include, 1) The
485 previous winter NAO would stimulate the anomalous NAT SST pattern; 2) The NAT can ~~last~~persist
486 from previous winter to the following spring due to the thermal persistence of the SST; 3) The spring
487 NAT plays significant modulation on the circulation pattern over North China through

488 teleconnection wave ~~trains, which ultimately affects train, affecting~~ the spring dust activities over
 489 North China. It is seen from Table 2 that although ~~in the case of ENSO phase and NAO & ENSO-~~
 490 ~~phase,~~ the correlation coefficients of previous winter NATI and spring NATI are same ~~in the case of~~
 491 ~~ENSO- phase and NAO- & ENSO- phase.~~ However, the correlations between the NAOI and NATI
 492 is higher during NAO- & ENSO- phase (0.66) than ~~during~~ ENSO- phase (0.52), highlighting the ~~a~~
 493 ~~more significant rolecontribution~~ of NAO ~~on their influencing~~ NAT in the case of NAO- & ENSO-
 494 phase. ~~The above discussion illustrates the synergistic effect of NAO and ENSO on the dust~~
 495 ~~activities over North China.~~



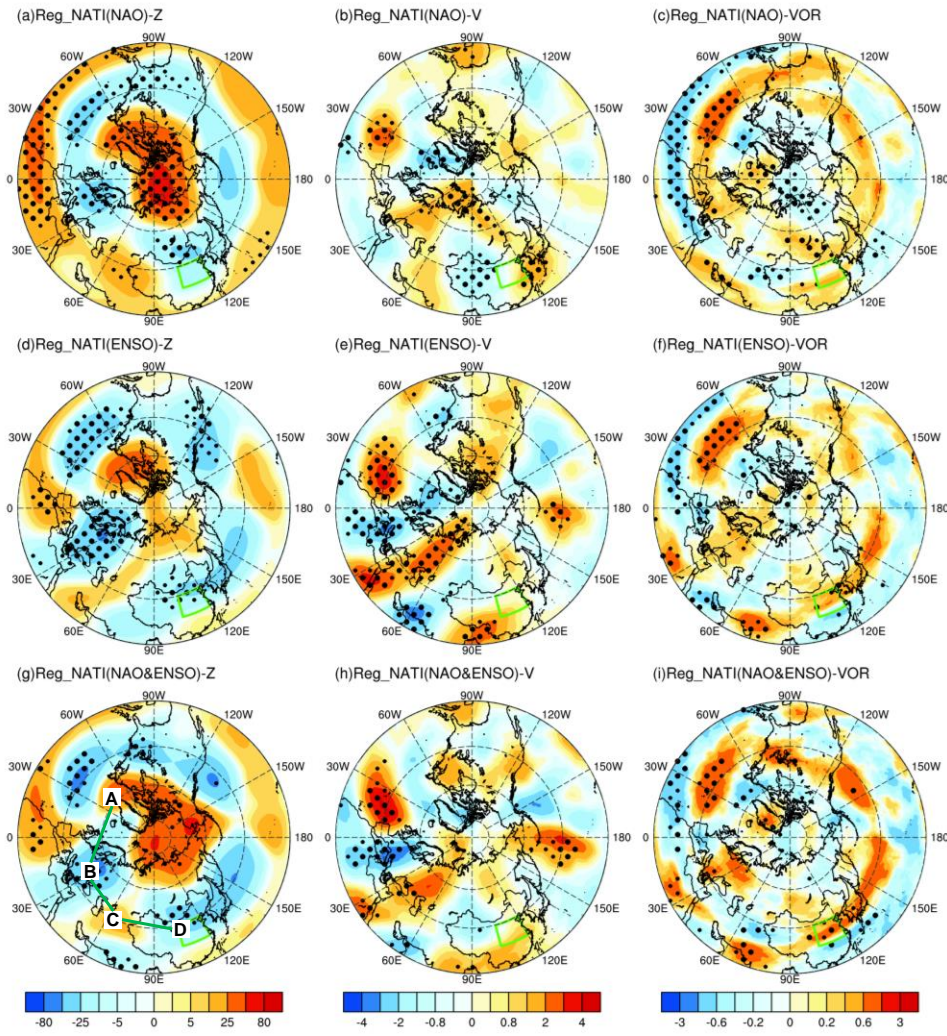
496
 497 **Figure 9.** Upper, correlation distributions of (a) winter NAOI with winter SST, (b) winter NATI
 498 with spring SST, and (c) winter NATI with SST_p during negative NAO phases. Middle-Lower, as
 499 in the upper, but during the negative ENSO phases and concurrent negative phases of NAO and
 500 ENSO, respectively. Thick and fine stippled areas are statistically significant at the 0.05 and 0.1
 501 level, respectively. The black box represents NATI.

502 **Table 2.** Correlation coefficients between the NAOI and NATI in different categories. * indicates
 503 statistically significant at the 0.1 level.

| Scenarios | DJF_NAO & DJF_NATI | DJF_NATI & MAM_NATI |
|--|--------------------|---------------------|
| NAO ⁻ phase | 0.41* | 0.51* |
| ENSO ⁻ phase | 0.52* | 0.69* |
| NAO ⁻ & ENSO ⁻ phase | 0.66* | 0.69* |

504 ~~The NAO preserves its anomalous signal within the tripole SST during the previous winter,~~
505 ~~and releases the anomalous signal in the following spring.~~ Given the distance across the ~~entire~~
506 Eurasian continent between the North Atlantic and North China, the role of teleconnection wave
507 ~~trains-train~~ is particularly important in influencing dust activities over North China. Figure 10a
508 ~~illustrates~~presents the geopotential height field at 200 hPa regressed onto the spring NATI during
509 ~~the~~ negative NAO case. This reveals a pronounced north-south reversed dipole pattern in the North
510 Atlantic, i.e., negative over Azores and positive over Iceland, representing a typical negative NAO
511 structure (Wallace and Gutzler, 1981; Li and Wang, 2003). ~~Meanwhile~~Additionally, a negative-
512 positive-negative~~positive~~ teleconnection wave-~~train~~ structure centered around eastern Europe,
513 Middle East, and North China is observed, suggesting that ~~the~~ disturbance energy propagates
514 downstream from the North Atlantic through waveguide effects, ~~leading to anticyclonic circulation~~
515 ~~anomalies in North China. Similar. The~~ teleconnection wave-train~~propagation~~ characteristics are
516 also observed in the 200 hPa meridional wind and vorticity fields (Figures 10b-c). During the
517 negative ENSO case, modulated by the NATI, ~~analogous~~similar teleconnection structures are also
518 seen in the circulation field (Figures 10d-f). Notably, when both the NAO and ENSO are ~~both~~-in
519 their negative phases, the correlation patterns of the teleconnection structure ~~reflected~~are similar,
520 however the anomalies over North China is enhanced, showing significant anomalies in the
521 ~~circulation~~vorticity field ~~is more pronounced than when only one factor is dominated~~ (Figures 10g-
522 i), confirming ~~the~~their synergistic effects ~~of both factors~~ on the circulation processes affecting dust
523 activities in North China.

524

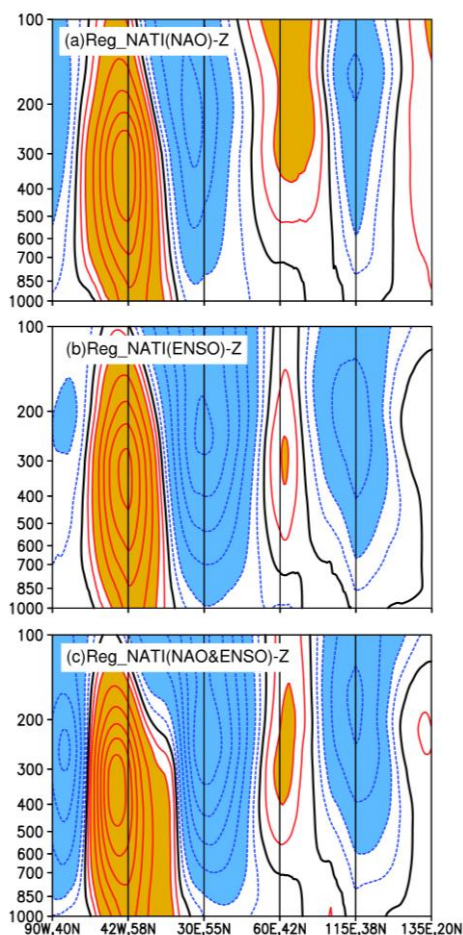


525

526 **Figure 10.** Upper, regression distribution of spring NATI against the spring (a) geopotential height
 527 (unit: gpm), (b) meridional wind (unit: $\text{m}\cdot\text{s}^{-1}$), and (c) vorticity (unit: $10^{-5}\cdot\text{m}\cdot\text{s}^{-1}$) at 200 hPa during
 528 the negative NAO phase. Middle-lower, as in the upper, but during the negative ENSO phases and
 529 concurrent negative phases of NAO and ENSO, respectively. The green box represents North China.
 530 Regression fields have multiplied by -1. (to facilitate a direct comparison between the
 531 NAO&ENSO associated circulation anomalies and the climatology). Thick and fine stippled areas
 532 are statistically significant at the 0.05 and 0.1 level, respectively.

533 To further examine the impact mechanisms of NAO and ENSO on ~~the~~ spring dust activities in
 534 North China, based on the propagation characteristics of the teleconnection wave ~~train~~
 535 Figure 10, the cross-section distribution of ~~cross-section of~~ the geopotential height field is presented
 536 (Figure 11). When both Under the scenarios where either the NAO and/or ENSO are is in their
 537 negative phases phase, the NATI anomalies correspond to the teleconnection wave ~~train~~
 538 from the upper to lower troposphere, which is specifically characterized by a negative-positive-
 539 negative-positive tripole teleconnection pattern. This wave train propagates from the North Atlantic,
 540 traversing centered around eastern Europe and, Middle East, and North China (Figures 11 a-b). This

541 wave-train propagate across Eurasian continent, ultimately influencing circulation processes
 542 associated with the dust activities over North China. Furthermore, the analysis of cross-section at
 543 different levels of the troposphere reveals that under the negative NAO and ENSO situations, the
 544 teleconnection wave-train excited by the NATI exhibits quasi-barotropic features, with this the
 545 anomalous structure being primarily concentrated in the middle-upper troposphere. When both the
 546 NAO and ENSO are simultaneously in their negative phases, the intensity and scope of the
 547 teleconnection wave-train are significantly enhanced and expanded compared to the influence of a
 548 single factor (Figure 11c), demonstrating synergistic effects.

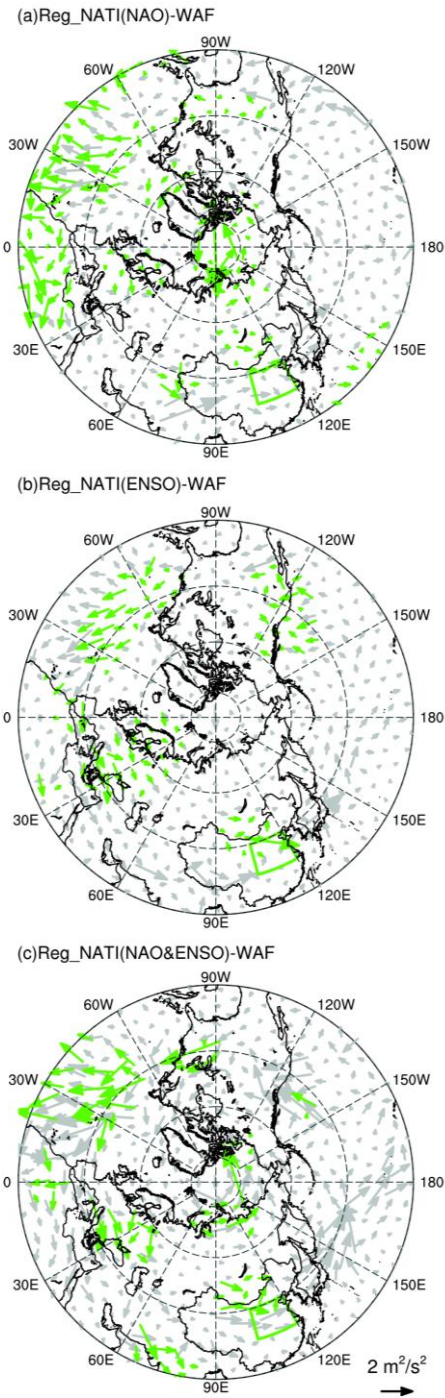


549
 550 **Figure 11.** Vertical section of regression of spring NATI against the geopotential height along the
 551 solid line labeled A (42°W, 58°N), B (30°E, 55°N), C (60°E, 42°N), and D (115°E, 38°N) in Figure
 552 10g for (a) negative NAO case in the previous winter. (b)-(c) as in (a), but during the negative ENSO
 553 case and co-occurring negative phases of NAO and ENSO, respectively (unit: gpm). Regression
 554 fields have multiplied by -1. (to facilitate a direct comparison between the NAO&ENSO associated
 555 circulation anomalies and the climatology). Shading indicates the absolute value is greater than 10
 556 gpm.

557 To provide a more comprehensive analysis of the transport process of disturbance energy in
 558 the atmosphere, the horizontal distribution of the WAF associated with spring NATI variations is

559 ~~further~~ examined. Under the ~~scenario that~~scenarios where either the NAO or ENSO is in ~~their~~the
560 negative ~~phases,~~phase, the WAF can be clearly observed ~~to originate~~originating from the North
561 Atlantic, ~~traverse~~traversing the Eurasian continent, and ~~extend~~extending to ~~the~~ North China (Figures
562 12a-b). When both factors occur simultaneously, ~~not only is~~ the transport intensity of the WAF is
563 not only enhanced, but its impact range on ~~the~~ dust activities in North China is also broadened
564 (Figure 12c). Through the analysis of teleconnection wave ~~trains-~~train and WAF, it is determined
565 that the synergistic effects not only enhance the disturbance intensity in the atmosphere, but also
566 expand impacted extent, thereby promoting the occurrence ~~and development~~ of spring dust activities
567 in North China. The enhancement and expansion of atmospheric disturbances may be related to
568 large-scale circulation anomalies and local climate condition ~~changes~~variations induced by the
569 synergistic effects of the NAO and ENSO, which in turn affect the transport and deposition
570 processes of dust.

571



572

573 **Figure 12.** As in Figure 10, but for the regression distribution of spring NATI against the T-N wave
 574 activity flux (units: $\text{m}^2 \cdot \text{s}^{-2}$). The green box represents North China. Regression fields have
 575 multiplied by -1. (to facilitate a direct comparison between the NAO&ENSO associated circulation
 576 anomalies and the climatology). Green arrows are statistically significant at the 0.1 level.

577 4. Conclusions and discussions

578 Although North China is not the primary dust source, dust activities are notably active during

579 spring in this region. This study highlights that the previous winter NAO and ENSO exert essential
580 influences on the following spring dust activities in North China. Their impacts are asymmetric,
581 manifesting only when both of them are in their negative phases. Furthermore, the results indicate
582 that NAO and ENSO in ~~the~~their negative ~~phase~~phases have synergistic effects on the spring dust
583 activities in North China, promoting dust activities and with greater impacts than their sole effect.

584 Under the ~~regulatory~~ influence of the negative phases of ~~the~~ NAO and ENSO, ~~the~~ atmospheric
585 circulation in the troposphere from the lower to upper layers, exhibits significant anomalies. These
586 include variations in the upper-level zonal winds, mid-latitude trough-ridge systems, and
587 atmospheric circulation ~~over the WNP, and the SH~~ at the SLP. These variations promote the
588 occurrence ~~and development~~ of dust activities in North China. Simultaneously, accompanying
589 anomalies in the atmospheric circulation pattern also affect local meteorological factors, including
590 humidity and precipitation, which in turn impact ~~the~~ dust activities in North China. Notably, when
591 both the NAO and ENSO are in their negative phases, synergistic effects occur, making the
592 anomalies in atmospheric circulation from the lower to upper layers, ~~as well as variations in~~
593 ~~humidity~~ and ~~precipitation~~ local meteorological factors, more conducive to the occurrence of dust
594 events in North China. The impact of ~~the~~ NAO on the underlying SST pattern is predominantly
595 observed during its negative phase, elucidating why the NAO significantly influences dust activities
596 in North China only during its negative phase. Furthermore, when both the NAO and ENSO
597 ~~simultaneously manifest~~are in their negative phases, the teleconnection wave ~~trains~~-train and WAF
598 stimulated from the North Atlantic are more intense, thereby more effectively influencing dust
599 activities in North China. This indicates the synergistic effects of ~~the~~these two variabilities on dust
600 activities over North China.

601 In the process where the previous winter NAO ~~and ENSO affect~~influences the following spring
602 dust activities in North China, the ~~persistence of anomalous NAT over North Atlantic~~NAT plays ~~an~~
603 ~~important~~a crucial role. The NAO signal from the previous winter ~~NAO stores its signal can be~~
604 stored in the NAT and persist into spring. In spring, ~~the~~ NAT regulates the circulation pattern in
605 North China through teleconnection wave ~~trains~~-train, ultimately affecting ~~the~~ dust activities ~~over~~in
606 North China. The signal of previous winter ENSO can persist into spring, ~~due to the persistence of~~
607 ~~SST~~, and it ~~affect~~effects on the dust activities in North China mainly through two pathways: i.e.,
608 directly ~~influencing~~influence the dust activities ~~in North China~~ by affecting the circulation
609 anomalies over the WNP, and ~~playing a~~facilitating ~~role in~~the process whereof which the NAO
610 excites NAT, thereby affecting the dust activities in North China. This provides a plausible

611 explanation for why the previous winter NAO and ENSO exert synergistic effects on the following
612 spring dust activities in North China.

613 This study investigated the impacts of NAO and ENSO on ~~the~~ dust activities in North China
614 and the ~~involved~~associated physical processes, indicating that one season ahead signals provide as
615 the useful predictors for spring dust activities in North China. Future work will focus on developing
616 a prediction model using the NAO and ENSO as predictors and validating its prediction
617 effectiveness. ~~Additionally, as previous studies have highlighted strong interdecadal variations in~~
618 ~~both~~The present work mainly focuses the NAO and ENSO (e.g., Woollings et al., 2015; Wang et al.,
619 2023; Feng et al., 2024), it is of interest to further detect whether the synergistic effects interannual
620 modulation of NAO and ENSO on the dust ~~activity~~activities over North China ~~experience~~
621 interdecadal variations. However, due to the availability of dataset, the potential impacts of the
622 interdecadal variability of the NAO and ENSO on, however, the NAO and ENSO (Woollings et al.,
623 2015; Feng et al., 2024), as well as dust activities have not been discussed in this over North China,
624 bear strong interdecadal variations, long-term datasets are needed to further explore their impacts
625 on the dust activities. The present study ~~Simultaneously~~ focuses on the period 1979-2022, due to
626 the longevity of the MERRA-2 dust content dataset. There are only 7 co-occurrence years of
627 negative NAO and ENSO, which take up to 17% of the whole study period. It is noted that the co-
628 occurrence events are not as many as either the negative NAO or ENSO, thus a significance level
629 of 0.1 is displayed. It is worthy to examine their joint impacts by employing longer datasets or
630 models outputs, to further explore their synergistic effects and any possible variations in their
631 modulations. Moreover, as reported that the state-of-art models can reproduce the individual impact
632 of NAO and ENSO on ~~the~~ dust activities in North China (Yang et al., 2022), whether their synergistic
633 effects on the dust activities could be well simulated, requiring further researches. ~~Additionally,~~
634 ~~previous~~Additionally, the potential impacts of interdecadal signals, such as the AMO, on dust
635 activities in China is not discussed. Future work will investigate the interdecadal variations of dust
636 activities in China and their connection to interdecadal climatic variabilities. Previous studies have
637 indicated that the uncertainty in ENSO variability is likely to increase under the background of
638 global warming (Cai et al., 2021; Chen et al., 2024). Therefore, it is crucial to investigate the future
639 changes in the ~~NAO, as well as future change of its synergistic effects with the ENSO on the dust~~
640 ~~activities, to better understand the plausible trends of future dust activities in North China~~. The
641 ~~present study is focused to period 1979-2022, due to the longevity of the MERRA-2 dust aerosol~~.
642 ~~There are only 7 co-occurrence years of negative NAO and ENSO. The co-occurrence of negative~~
643 ~~NAO and ENSO takes up to 17% of the whole study period. To be noted is that the sample are not~~

644 ~~long enough, it is worthy to examine their joint impacts by employing longer datasets or models~~
645 ~~outputs, to further detect their synergistic effects as well as any possible variations in their~~
646 ~~modulations. This study did not discuss the potential impacts of interdecadal signals, such as the~~
647 ~~AMO, on dust activities in China. The interdecadal variations of dust activities over China as well~~
648 ~~as its connection to the interdecadal climatic variabilities will be discussed in future work.~~ENSO
649 and its synergistic effects with NAO on the dust activities over China, to better understand the
650 plausible trends of future dust activities in North China.

651

652 **Code and data availability.** The MERRA-2 dust ~~aerosol~~ content dataset can be downloaded from
653 <https://disc.gsfc.nasa.gov/datasets?project=MERRA-2> (last access: 722 July 2024). The
654 atmospheric reanalysis datasets, ~~including wind, geopotential height, and sea level pressure,~~
655 ~~specific humidity, precipitation, and vorticity field~~ can be downloaded from
656 <https://cds.climate.copernicus.eu/#!/search?text=ERA5&type=dataset> (last access: 722 July 2024).
657 The oceanic reanalysis data can be downloaded from <https://www.metoffice.gov.uk/hadobs/hadisst>
658 (last access: 722 July 2024). The NAO indices defined by Li and Wang can be downloaded from
659 <http://lijianping.cn/dct/page/65610> (last access: 722 July 2024). The NAO indices produce by
660 Hurrell and Jones can be downloaded from [https://climatedataguide.ucar.edu/climate-data/hurrell-](https://climatedataguide.ucar.edu/climate-data/hurrell-north-atlantic-oscillation-nao-index-pc-based)
661 [north-atlantic-oscillation-nao-index-pc-based](https://climatedataguide.ucar.edu/climate-data/hurrell-north-atlantic-oscillation-nao-index-pc-based) (last access: 722 July 2024) and
662 <https://crudata.uea.ac.uk/cru/data/nao> (last access: 722 July 2024), respectively. The ENSO indices
663 can be downloaded from <https://psl.noaa.gov/data/timeseries/monthly/NINO34> (last access: 722
664 July 2024). Our results can be made available upon request.

665

666 **Author contributions.** JF and FLX conceptualized and designed the research. FLX and JF
667 synthesized and analyzed the data. FLX, SW, YL, and JF produced the figures. FLX and SW
668 contributed to the dataset's retrieval. All the authors discussed the results and wrote the paper.

669

670 **Competing interests.** The authors declare that they have no conflict of interest.

671

672 **Disclaimer.** Publisher's note: Copernicus Publications remains neutral with regard to jurisdictional
673 claims in published maps and institutional affiliations.

674 **Acknowledgements.** The authors would like to thank the Editor Marco Gaetani and two anonymous
675 reviewers for their useful comments and suggestions that contributed to improving the manuscript.
676 This work was jointly supported by the National Natural Science Foundation of China (42222501)
677 and the BNU-FGS Global Environmental Change Program (No. 2023-GC-ZYTS-03). This work
678 was supported by the National Key Scientific and Technological Infrastructure project “Earth
679 System Numerical Simulation Facility” (EarthLab).

680

681

References

- 682 Abid, M. A., Kucharski, F., Molteni, F., Kang, I.-S., Tompkins, A. M., and Almazroui, M.: Separating the Indian and
683 Pacific Ocean Impacts on the Euro-Atlantic Response to ENSO and Its Transition from Early to Late Winter, *J.*
684 *Climate*, 34, 1531–1548, <https://doi.org/10.1175/JCLI-D-20-0075.1>, 2021.
- 685 Achakulwisut, P., Shen, L., and Mickley, L. J.: What Controls Springtime Fine Dust Variability in the Western United
686 States? Investigating the 2002–2015 Increase in Fine Dust in the U.S. Southwest, *J. Geophys. Res.-Atmos.*, 122,
687 <https://doi.org/10.1002/2017JD027208>, 2017.
- 688 Ayarzagüena, B., Ineson, S., Dunstone, N. J., Baldwin, M. P., and Scaife, A. A.: Intraseasonal Effects of El Niño–
689 Southern Oscillation on North Atlantic Climate, *J. Climate*, 31, 8861–8873, [https://doi.org/10.1175/JCLI-D-18-](https://doi.org/10.1175/JCLI-D-18-0097.1)
690 [0097.1](https://doi.org/10.1175/JCLI-D-18-0097.1), 2018.
- 691 Cai, W. J., Santoso, A., Collins, M., Dewitte, B., Karamperidou, C., Kug, J.-S., Lengaigne, M., McPhaden, M. J.,
692 Stuecker, M. F., Taschetto, A. S., Timmermann, A., Wu, L. X., Yeh, S.-W., Wang, G. J., Ng, B., Jia, F., Yang, Y.,
693 Ying, J., Zheng, X. T., Bayr, T., Brown, J. R., Capotondi, A., Cobb, K. M., Gan, B. L., Geng, T., Ham, Y.-G.,
694 Jin, F. F., Jo, H.-S., Li, X. C., Lin, X. P., McGregor, S., Park, J.-H., Stein, K., Yang, K., Zhang, L., and Zhong,
695 W. X.: Changing El Niño–Southern Oscillation in a warming climate, *Nat. Rev.-Earth Environ.*, 2, 628–644,
696 <https://doi.org/10.1038/s43017-021-00199-z>, 2021.
- 697 Chen, S. F., Wu, R. G., and Chen, W.: Strengthened Connection between Springtime North Atlantic Oscillation and
698 North Atlantic Tripole SST Pattern since the Late 1980s, *J. Climate*, 35, 2007–2022,
699 <https://doi.org/10.1175/JCLI-D-19-0628.1>, 2020.
- 700 Chen, S. F., Chen W., Xie, S. P., Yu, B., Wu, R. G., Wang, Z. B., Lan, X. Q., and Graf, H.: Strengthened impact of
701 boreal winter North Pacific Oscillation on ENSO development in warming climate, *npj Climate and*
702 *Atmospheric Science*, 7, 69, <https://doi.org/10.1038/s41612-024-00615-3>, 2024.
- 703 Chen, S. Y., Zhao, D., Huang, J. P., He, J. Q., Chen, Y., Chen, J. Y., Bi, H. R., Lou, G. T., Du, S. K., Zhang, Y., and
704 Yang, F.: Mongolia Contributed More than 42% of the Dust Concentrations in Northern China in March and
705 April 2023, *Adv. Atmos. Sci.*, 40, 1549–1557, <https://doi.org/10.1007/s00376-023-3062-1>, 2023.
- 706 Cressman, G. P.: An operational objective analysis system, *Mon. Weather Rev.*, 87, 367–374,
707 [https://doi.org/10.1175/1520-0493\(1959\)087<0367:AOOAS>2.0.CO;2](https://doi.org/10.1175/1520-0493(1959)087<0367:AOOAS>2.0.CO;2), 1959.
- 708 Csavina, J., Field, J., Félix, O., Corral-Avitia, A. Y., Sáez, A. E., and Betterton, E. A.: Effect of wind speed and
709 relative humidity on atmospheric dust concentrations in semi-arid climates, *Sci. Total Environ.*, 487, 82–90,
710 <https://doi.org/10.1016/j.scitotenv.2014.03.138>, 2014.
- 711 Ding, R. Q., Nnamchi, H. C., Yu, J. Y., Li, T., Sun, C., Li, J. P., Tseng, Y., Li, X. C., Xie, F., Feng, J., Ji, K., and Li,
712 X. M.: North Atlantic oscillation controls multidecadal changes in the North Tropical Atlantic–Pacific
713 connection, *Nat. Commun.*, 14, 862, <https://doi.org/10.1038/s41467-023-36564-3>, 2023.
- 714 Fan, K., Xie, Z. M., Wang, H. J., Xu, Z. Q., and Liu, J. P.: Frequency of spring dust weather in North China linked
715 to sea ice variability in the Barents Sea, *Clim. Dyn.*, 51, 4439–4450, [https://doi.org/10.1007/s00382-016-3515-](https://doi.org/10.1007/s00382-016-3515-7)
716 [7](https://doi.org/10.1007/s00382-016-3515-7), 2018.
- 717 Feldstein, S. B.: The dynamics of NAO teleconnection pattern growth and decay, *Q. J. Roy. Meteor. Soc.*, 129, 901–
718 924, <https://doi.org/10.1256/qj.02.76>, 2003.
- 719 Feng, J. and Li, J. P.: Influence of El Niño Modoki on spring rainfall over south China, *J. Geophys. Res.-Atmos.*,
720 116, D13102, <https://doi.org/10.1029/2010JD015160>, 2011.
- 721 Feng, J., Li, J. P., Liao, H., and Zhu, J. L.: Simulated coordinated impacts of the previous autumn North Atlantic
722 Oscillation (NAO) and winter El Niño on winter aerosol concentrations over eastern China, *Atmos. Chem.*
723 *Phys.*, 19, 10787–10800, <https://doi.org/10.5194/acp-19-10787-2019>, 2019.

724 Feng, J., Wang, S., and Li, J. P.: Strengthened ENSO amplitude contributed to regime shift in the Hadley circulation.
725 *Geophys. Res. Lett.*, 51, e2023GL106006. <https://doi.org/10.1029/2023GL106006>, 2024.

726 Feng, J., Zhu, J. L., Li, J. P., and Liao, H.: Aerosol concentrations variability over China: two distinct leading modes,
727 *Atmos. Chem. Phys.*, 20, 9883–9893, <https://doi.org/10.5194/acp-20-9883-2020>, 2020.

728 Gelaro, R., McCarty, W., Suárez, M. J., Todling, R., Molod, A., Takacs, L., Randles, C. A., Darmenov, A., Bosilovich,
729 M. G., Reichle, R., Wargan, K., Coy, L., Cullather, R., Draper, C., Akella, S., Buchard, V., Conaty, A., Da Silva,
730 A. M., Gu, W., Kim, G.-K., Koster, R., Lucchesi, R., Merkova, D., Nielsen, J. E., Partyka, G., Pawson, S.,
731 Putman, W., Rienecker, M., Schubert, S. D., Sienkiewicz, M., and Zhao, B.: The Modern-Era Retrospective
732 Analysis for Research and Applications, Version 2 (MERRA-2), *J. Climate*, 30, 5419–5454,
733 <https://doi.org/10.1175/JCLI-D-16-0758.1>, 2017.

734 Gong, S. L., Zhang, X. Y., Zhao, T. L., Zhang, X. B., Barrie, L. A., McKendry, I. G., and Zhao, C. S.: A Simulated
735 Climatology of Asian Dust Aerosol and Its Trans-Pacific Transport. Part II: Interannual Variability and Climate
736 Connections, *J. Climate*, 19, 104–122, <https://doi.org/10.1175/JCLI3606.1>, 2006.

737 Guo, Y., Li, J. P., and Li, Y.: A Time-Scale Decomposition Approach to Statistically Downscale Summer Rainfall
738 over North China, *J. Climate*, 25, 572–591, <https://doi.org/10.1175/JCLI-D-11-00014.1>, 2012.

739 Hersbach, H., Bell, B., Berrisford, P., Hirahara, S., Horányi, A., Muñoz-Sabater, J., Nicolas, J., Peubey, C., Radu,
740 R., Schepers, D., Simmons, A., Soci, C., Abdalla, S., Abellan, X., Balsamo, G., Bechtold, P., Biavati, G., Bidlot,
741 J., Bonavita, M., De Chiara, G., Dahlgren, P., Dee, D., Diamantakis, M., Dragani, R., Flemming, J., Forbes, R.,
742 Fuentes, M., Geer, A., Haimberger, L., Healy, S., Hogan, R. J., Hólm, E., Janisková, M., Keeley, S., Laloyaux,
743 P., Lopez, P., Lupu, C., Radnoti, G., De Rosnay, P., Rozum, I., Vamborg, F., Villaume, S., and Thépaut, J.: The
744 ERA5 global reanalysis, *Q. J. Roy. Meteor. Soc.*, 146, 1999–2049, <https://doi.org/10.1002/qj.3803>, 2020.

745 Huang, J., Li, Y., Fu, C., Chen, F., Fu, Q., Dai, A., Shinoda, M., Ma, Z., Guo, W., Li, Z., Zhang, L., Liu, Y., Yu, H.,
746 He, Y., Xie, Y., Guan, X., Ji, M., Lin, L., Wang, S., Yan, H., and Wang, G.: Dryland climate change: Recent
747 progress and challenges, *Rev. Geophys.*, 55, 719–778, <https://doi.org/10.1002/2016RG000550>, 2017.

748 Huang, J. P., Liu, J. J., Chen, B., and Nasiri, S. L.: Detection of anthropogenic dust using CALIPSO lidar
749 measurements, *Atmos. Chem. Phys.*, 15, 11653–11665, <https://doi.org/10.5194/acp-15-11653-2015>, 2015.

750 Huang, Y. H., Liu, X. D., Yin, Z., and An, Z. S.: Global Impact of ENSO on Dust Activities with Emphasis on the
751 Key Region from the Arabian Peninsula to Central Asia, *J. Geophys. Res.-Atmos.*, 126, e2020JD034068,
752 <https://doi.org/10.1029/2020JD034068>, 2021.

753 Hurrell, J. W.: Decadal Trends in the North Atlantic Oscillation: Regional Temperatures and Precipitation, *Science*,
754 269, 676–679, <https://doi.org/10.1126/science.269.5224.676>, 1995.

755 Ji, L. Q. and Fan, K.: Climate prediction of dust weather frequency over northern China based on sea-ice cover and
756 vegetation variability, *Clim. Dyn.*, 53, 687–705, <https://doi.org/10.1007/s00382-018-04608-w>, 2019.

757 Jia, X. J., Derome, J., and Lin, H.: Comparison of the Life Cycles of the NAO Using Different Definitions, *J. Climate*,
758 20, 5992–6011, <https://doi.org/10.1175/2007JCLI1408.1>, 2007.

759 Jiang, W. P., Huang, G., Huang, P., Wu, R. G., Hu, K. M., and Chen, W.: Northwest Pacific Anticyclonic Anomalies
760 during Post-El Niño Summers Determined by the Pace of El Niño Decay, *J. Climate*, 32, 3487–3503,
761 <https://doi.org/10.1175/JCLI-D-18-0793.1>, 2019.

762 Jiménez-Esteve, B. and Domeisen, D. I. V.: The Tropospheric Pathway of the ENSO–North Atlantic Teleconnection,
763 *J. Climate*, 31, 4563–4584, <https://doi.org/10.1175/JCLI-D-17-0716.1>, 2018.

764 Jones, P. D., Jonsson, T., and Wheeler, D.: Extension to the North Atlantic Oscillation using early instrumental
765 pressure observations from Gibraltar and South-West Iceland. *Int. J. Climatol.*, 17, 1433–1450,
766 [https://doi.org/10.1002/\(SICI\)1097-0088\(19971115\)17:13<1433::AID-JOC203>3.0.CO;2-P](https://doi.org/10.1002/(SICI)1097-0088(19971115)17:13<1433::AID-JOC203>3.0.CO;2-P), 1997.

767 Kang, L. T., Huang, J. P., Chen, S. Y., and Wang, X.: Long-term trends of dust events over Tibetan Plateau during
768 1961-2010, *Atmos. Environ.*, 125, 188-198, <https://doi.org/10.1016/j.atmosenv.2015.10.085>, 2016.

769 Kim, H. and Choi, M.: Impact of soil moisture on dust outbreaks in East Asia: Using satellite and assimilation data,
770 *Geophys. Res. Lett.*, 42, 2789–2796, <https://doi.org/10.1002/2015GL063325>, 2015.

771 Kim, S. and Kug, J.: What Controls ENSO Teleconnection to East Asia? Role of Western North Pacific Precipitation
772 in ENSO Teleconnection to East Asia, *J. Geophys. Res.-Atmos.*, 123, <https://doi.org/10.1029/2018JD028935>,
773 2018.

774 Kok, J. F., Storelvmo, T., Karydis, V. A., Adebisi, A. A., Mahowald, N. M., Evan, A. T., He, C. L., and Leung, D.
775 M.: Mineral dust aerosol impacts on global climate and climate change, *Nat. Rev.-Earth Environ.*, 4, 71–86,
776 <https://doi.org/10.1038/s43017-022-00379-5>, 2023.

777 Li, J. P., and Wang, J. X. L.: A new North Atlantic Oscillation index and its variability, *Adv. Atmos. Sci.*, 20, 661–
778 676, <https://doi.org/10.1007/BF02915394>, 2003.

779 Li, J. P., Zheng, F., Sun, C., Feng, J., and Wang, J.: Pathways of Influence of the Northern Hemisphere Mid-high
780 Latitudes on East Asian Climate: A Review, *Adv. Atmos. Sci.*, 36, 902–921, <https://doi.org/10.1007/s00376-019-8236-5>, 2019.

782 Li, Y., Xu, F. L., Feng, J., Du, M. Y., Song, W. J., Li, C., and Zhao, W. J.: Influence of the previous North Atlantic
783 Oscillation (NAO) on the spring dust aerosols over North China, *Atmos. Chem. Phys.*, 23, 6021–6042,
784 <https://doi.org/10.5194/acp-23-6021-2023>, 2023.

785 Liu, X. D., Yin, Z., Zhang, X. Y., and Yang, X. C.: Analyses of the spring dust storm frequency of northern China in
786 relation to antecedent and concurrent wind, precipitation, vegetation, and soil moisture conditions, *J. Geophys.*
787 *Res.-Atmos.*, 109, 2004JD004615, <https://doi.org/10.1029/2004JD004615>, 2004.

788 López-Parages, J., Rodríguez-Fonseca, B., and Terray, L.: A mechanism for the multidecadal modulation of ENSO
789 teleconnection with Europe, *Clim. Dyn.*, 45, 867–880, <https://doi.org/10.1007/s00382-014-2319-x>, 2015.

790 Lou, S. J., Russell, L. M., Yang, Y., Xu, L., Lamjiri, M. A., DeFlorio, M. J., Miller, A. J., Ghan, S. J., Liu, Y., and
791 Singh, B.: Impacts of the East Asian Monsoon on springtime dust concentrations over China, *J. Geophys. Res.-*
792 *Atmos.*, 121, 8137–8152, <https://doi.org/10.1002/2016JD024758>, 2016.

793 Lou, S. J., Russell, L. M., Yang, Y., Liu, Y., Singh, B., and Ghan, S. J.: Impacts of interactive dust and its direct
794 radiative forcing on interannual variations of temperature and precipitation in winter over East Asia, *J. Geophys.*
795 *Res.-Atmos.*, 122, 8761–8780, <https://doi.org/10.1002/2017JD027267>, 2017.

796 McPhaden, M. J. and Zhang, X. B.: Asymmetry in zonal phase propagation of ENSO sea surface temperature
797 anomalies, *Geophys. Res. Lett.*, 36, 2009GL038774, <https://doi.org/10.1029/2009GL038774>, 2009.

798 Pan, L. L.: Observed positive feedback between the NAO and the North Atlantic SSTA tripole, *Geophys. Res. Lett.*,
799 32, 2005GL022427, <https://doi.org/10.1029/2005GL022427>, 2005.

800 Prospero, J. M., Nees, R. T., and Uematsu, M.: Deposition rate of particulate and dissolved aluminum derived from
801 saharan dust in precipitation at Miami, Florida, *J. Geophys. Res.-Atmos.*, 92, 14723–14731,
802 <https://doi.org/10.1029/JD092iD12p14723>, 1987.

803 Rayner, N. A., Parker, D. E., Horton, E. B., Folland, C. K., Alexander, L. V., Rowell, D. P., Kent, E. C., and Kaplan,
804 A.: Global analyses of sea surface temperature, sea ice, and night marine air temperature since the late
805 nineteenth century, *J. Geophys. Res.-Atmos.*, 108, 2002JD002670, <https://doi.org/10.1029/2002JD002670>,
806 2003.

807 Song, L. Y., Chen, S. F., Chen, W., Guo, J. P., Cheng, C. L., and Wang, Y.: Distinct evolutions of haze pollution from
808 winter to following spring over the North China Plain: Role of the North Atlantic sea surface temperature
809 anomalies. *Atmos. Chem. Phys.*, 22, 1669–1688, <https://doi.org/10.5194/acp-22-1669-2022>, 2022.

810 Su, J. Z., Zhang, R. H., Li, T., Rong, X. Y., Kug, J., and Hong, C.: Causes of the El Niño and La Niña Amplitude
811 Asymmetry in the Equatorial Eastern Pacific, *J. Climate*, 23, 605–617, <https://doi.org/10.1175/2009JCLI2894.1>,
812 2010.

813 Sung, M., Lim, G., and Kug, J.: Phase asymmetric downstream development of the North Atlantic Oscillation and
814 its impact on the East Asian winter monsoon, *J. Geophys. Res.-Atmos.*, 115, 2009JD013153,
815 <https://doi.org/10.1029/2009JD013153>, 2010.

816 Takaya, K. and Nakamura, H.: A Formulation of a Phase-Independent Wave-Activity Flux for Stationary and
817 Migratory Quasigeostrophic Eddies on a Zonally Varying Basic Flow, *J. Atmospheric Sci.*, 58, 608–627,
818 [https://doi.org/10.1175/1520-0469\(2001\)058<0608:AFOAPI>2.0.CO;2](https://doi.org/10.1175/1520-0469(2001)058<0608:AFOAPI>2.0.CO;2), 2001.

819 Trenberth, K. E.: The Definition of El Niño, *B. Am. Meteorol. Soc.*, 78, 2771–2777, [https://doi.org/10.1175/1520-0477\(1997\)078<2771:TDOENO>2.0.CO;2](https://doi.org/10.1175/1520-0477(1997)078<2771:TDOENO>2.0.CO;2), 1997.

820
821 Wallace, J. M. and Gutzler, D. S.: Teleconnections in the Geopotential Height Field during the Northern Hemisphere
822 Winter, *Mon. Weather Rev.*, 109, 784–812, [https://doi.org/10.1175/1520-0493\(1981\)109<0784:TITGHF>2.0.CO;2](https://doi.org/10.1175/1520-0493(1981)109<0784:TITGHF>2.0.CO;2), 1981.

823
824 Wang, B., Wu, R. G., and Fu, X. H.: Pacific–East Asian Teleconnection: How Does ENSO Affect East Asian Climate?
825 *J. Climate*, 13, 1517–1536, [https://doi.org/10.1175/1520-0442\(2000\)013<1517:PEATHD>2.0.CO;2](https://doi.org/10.1175/1520-0442(2000)013<1517:PEATHD>2.0.CO;2), 2000.

826 Wang, T. H., Tang, J. Y., Sun, M. X., Liu, X. W., Huang, Y. X., Huang, J. P., Han, Y., Cheng, Y. F., Huang, Z. W., and
827 Li, J. M.: Identifying a transport mechanism of dust aerosols over South Asia to the Tibetan Plateau: A case
828 study, *Sci. Total Environ.*, 758, 11, <https://doi.org/10.1016/j.scitotenv.2020.143714>, 2021.

829 Wang, X., Huang, J. P., Ji, M. X., and Higuchi, K.: Variability of East Asia dust events and their long-term trend,
830 *Atmos. Environ.*, 42, <https://doi.org/10.1016/j.atmosenv.2007.07.046>, 2008

831 Woollings, T., Franzke, C., Hodson, D. L. R., Dong, B., Barnes, E. A., Raible, C. C., and Pinto, J. G.: Contrasting
832 interannual and multidecadal NAO variability, *Clim. Dyn.*, 45, 539–556, <https://doi.org/10.1007/s00382-014-2237-y>, 2015.

833
834 Wu, J., Kurosaki, Y., Shinoda, M., and Kai, K.: Regional Characteristics of Recent Dust Occurrence and Its
835 Controlling Factors in East Asia, *Sola*, 12, 187–191, <https://doi.org/10.2151/sola.2016-038>, 2016.

836 Wu, R. G. and Chen, S. F.: What Leads to Persisting Surface Air Temperature Anomalies from Winter to Following
837 Spring over Mid- to High-Latitude Eurasia? *J. Climate*, 33, 5861–5883, <https://doi.org/10.1175/JCLI-D-19-0819.1>, 2020.

838
839 Wu, Z. W., Wang, B., Li, J. P., and Jin, F. F.: An empirical seasonal prediction model of the east Asian summer
840 monsoon using ENSO and NAO, *J. Geophys. Res.-Atmos.*, 114, 2009JD011733,
841 <https://doi.org/10.1029/2009JD011733>, 2009.

842 Wu, Z. W., Li, J. P., Jiang, Z. H., He, J. H., and Zhu, X. Y.: Possible effects of the North Atlantic Oscillation on the
843 strengthening relationship between the East Asian Summer monsoon and ENSO, *Int. J. Climatol.*, 32, 794–800,
844 <https://doi.org/10.1002/joc.2309>, 2012.

845 Yang, Y., Zeng, L. Y., Wang, H. L., Wang, P. Y., and Liao, H.: Dust pollution in China affected by different spatial
846 and temporal types of El Niño, *Atmos. Chem. Phys.*, 22, 14489–14502, <https://doi.org/10.5194/acp-22-14489-2022>, 2022.

847
848 Yu, Y., Notaro, M., Liu, Z. Y., Wang, F. Y., Alkolibi, F., Fadda, E., and Bakhrjy, F.: Climatic controls on the
849 interannual to decadal variability in Saudi Arabian dust activity: Toward the development of a seasonal dust
850 prediction model, *J. Geophys. Res.-Atmos.*, 120, 1739–1758, <https://doi.org/10.1002/2014JD022611>, 2015.

851 Zhang, R. H., Li, T. R., Wen, M., and Liu, L. K.: Role of intraseasonal oscillation in asymmetric impacts of El Niño
852 and La Niña on the rainfall over southern China in boreal winter, *Clim. Dyn.*, 45, 559–567,
853 <https://doi.org/10.1007/s00382-014-2207-4>, 2015.

-
- 854 Zhang, W. J., Li, J. P., and Jin, F. F.: Spatial and temporal features of ENSO meridional scales, *Geophys. Res. Lett.*,
855 36, 2009GL038672, <https://doi.org/10.1029/2009GL038672>, 2009.
- 856 Zhang, X. Y., Gong, S. L., Zhao, T. L., Arimoto, R., Wang, Y. Q., and Zhou, Z. J.: Sources of Asian dust and role of
857 climate change versus desertification in Asian dust emission, *Geophys. Res. Lett.*, 30, 2003GL018206,
858 <https://doi.org/10.1029/2003GL018206>, 2003.
- 859 Zhao, C. F., Yang, Y. K., Fan, H., Huang, J. P., Fu, Y. F., Zhang, X. Y., Kang, S. C., Cong, Z. Y., Letu, H., and Menenti,
860 M.: Aerosol characteristics and impacts on weather and climate over the Tibetan Plateau, *Natl. Sci. Rev.*, 7,
861 492–495, <https://doi.org/10.1093/nsr/nwz184>, 2020.
- 862 Zhao, Y., Huang, A. N., Zhu, X. S., Zhou, Y., and Huang, Y.: The impact of the winter North Atlantic Oscillation on
863 the frequency of spring dust storms over Tarim Basin in northwest China in the past half-century, *Environ. Res.*
864 *Lett.*, 8, 024026, <https://doi.org/10.1088/1748-9326/8/2/024026>, 2013.
- 865 Zheng, F., Li, J. P., Li, Y. J., Zhao, S., and Deng, D. F.: Influence of the Summer NAO on the Spring-NAO-Based
866 Predictability of the East Asian Summer Monsoon, *J. Appl. Meteorol. Clim.*, 55, 1459–1476,
867 <https://doi.org/10.1175/JAMC-D-15-0199.1>, 2016a.
- 868 Zheng, Y., Zhao, T. L., Che, H. Z., Liu, Y., Han, Y. X., Liu, C., Xiong, J., Liu, J. H., and Zhou, Y. K.: A 20-year
869 simulated climatology of global dust aerosol deposition, *Sci. Total Environ.*, 557–558, 861–868,
870 <https://doi.org/10.1016/j.scitotenv.2016.03.086>, 2016b.
- 871 Zhou, F., Shi, J., Liu, M. H., and Ren, H. C.: Linkage between the NAO and Siberian high events on the intraseasonal
872 timescale, *Atmos. Res.*, 281, 106478, <https://doi.org/10.1016/j.atmosres.2022.106478>, 2023.
- 873 Zhu, C. W., Wang, B., and Qian, W. H.: Why do dust storms decrease in northern China concurrently with the recent
874 global warming? *Geophys. Res. Lett.*, 35, 2008GL034886, <https://doi.org/10.1029/2008GL034886>, 2008.